Conditions for detection of ground deformation induced by conduit flow and evolution

F. Albino, Virginie Pinel, H. Massol, M. Collombet

JOURNAL OF GEOPHYSICAL RESEARCH, VOL. ???, XXXX, DOI:10.1029/,

Conditions for detection of ground deformation induced by conduit flow and evolution

F. Albino[1], V. Pinel[1], H. Massol[2] and M. Collombet[1]

F. Albino, ISTerre, CNRS, IRD, Université de Savoie, Campus scientifique, 73376 Le Bourget du Lac Cedex, FRANCE. (Fabien.Albino@univ-savoie.fr)

M. Collombet, ISTerre, CNRS, IRD, Université de Savoie, Campus scientifique, 73376 Le Bourget du Lac Cedex, FRANCE.

H. Massol, Laboratoire IDES, Département des Sciences de la Terre, Université Paris XI, 91405 Orsay Cedex, FRANCE.

V. Pinel, ISTerre, CNRS, IRD, Université de Savoie, Campus scientifique, 73376 Le Bourget du Lac Cedex, FRANCE.

[1]ISTerre, CNRS, IRD, Université de Savoie, Campus scientifique, 73376 Le Bourget du Lac Cedex, FRANCE.

[2]Lab. IDES, Département des Sciences de la Terre, Université Paris XI, 91405 Orsay Cedex, FRANCE.

Abstract. At mature andesitic volcanoes, magma can reach the surface through the same path for several eruptions thus forming a volcanic conduit. Due to degassing, cooling and crystallization, magma viscosity increase in the upper part of the conduit may induce the formation of a viscous plug. We conducted numerical simulations to quantify the deformation field caused by this plug emplacement and evolution. Stress continuity between Newtonian magma flow and elastic crust is considered. Plug emplacement causes a ground inflation correlated to a decrease of the magma discharge rate. A parametric study shows that surface displacements depend on three dimensionless numbers: the conduit aspect ratio (radius/length), the length ratio between the plug and the conduit and the viscosity contrast between the plug and the magma column. Larger displacements are obtained for high viscosity plugs emplaced in large aspect ratio conduits. We find that only tiltmeters or GPS located close the vent (a few hundred meters) might record the plug emplacement. At immediate proximity of the vent, plug emplacement might even dominate the deformation signal, over dome growth or magma reservoir pressurization effects. For given plug thicknesses and viscosity profiles, our model explain well the amplitude of tilt variations (from 1 to 25 μrad) measured at Montserrat and Mt. St. Helens. We also demonstrate that, at Montserrat, even if most of the tilt signal is due to shear stress induced by magma flow, pressurization beneath the plug account for 20 percent of the signal.

1. Introduction

Cyclic patterns of activity, with a succession of episodes of lava dome growth and quiescent periods, have been observed at many andesitic volcanoes, such as Soufrière Hills (Montserrat, 1995-present), Mt St Helens (USA, 1980-1986), Merapi (Philippines, 1768-1998), Unzen (Japan, 1990-1995) or Santiaguito (Guatemala, 1922-2000) [*Voight et al.*, 1999; *Swanson and Holcomb*, 1990; *Voight et al.*, 2000; *Nakada et al.*, 1999; *Harris et al.*, 2002]. Large fluctuations in discharge rate are correlated with fluctuations of various signals such as ground deformation, seismicity and gas emissions. For long-term cycles, (months to years), the mechanism invoked is pressure changes occurring within a magma reservoir [*Melnik and Sparks*, 2005]. In some volcanic areas such as Soufrière Hills, Mt St Helens or Merapi, improvement of volcanic monitoring, with acquisitions of high frequency and precise data, has permitted to identify cyclic patterns with a period of only a few hours, during phases of dome extrusion [*Voight et al.*, 1999]. Whereas cyclic deformation at long time-scales is attributed to magma reservoir dynamics, short time-scale variations are explained by the non-linear dynamics of magma flow in the volcanic conduit [*Denlinger and Hoblitt*, 1999; *Voight et al.*, 1999; *Wylie et al.*, 1999; *Lensky et al.*, 2008; *Collier and Neuberg*, 2006]. Intermediate cycles with periods of several weeks have been attributed to the capacitor effect of dykes connecting magma reservoirs and upper conduits [*Costa et al.*, 2007b]. Also, sudden events characteristic of andesitic volcanic activity, such as dome collapse, can induce rapid pressure changes within the magma reservoir [*Voight et al.*, 2006]. It follows that a combination of changes taking place at different levels of the magma plumbing system, causes the temporal evolution of volcanic activity. In order to improve eruption forecasting, it is required to study magma flow conditions in the volcanic conduit of andesitic volcanoes and how it affects the monitoring signals recorded at the surface.

Previous work [*Sparks*, 1997; *Melnik and Sparks*, 1999; *Barmin et al.*, 2002], focussing on changes of the physical properties of the ascending magma, has shown that gas loss and crystallization occur mainly within the last hundred of meters below the surface. Both mechanisms may induce a strong increase in magma viscosity of several orders of magnitude [*Shaw*, 1963; *Hess and Dingwell*, 1996; *Llewellin and Manga*, 2005]. For example, the viscosity of an andesitic magma at 900 °C containing 5 wt% is around 10^4 Pa.s, but can reach values of 10^{11} Pa.s if the magma is fully degassed [*Sparks*, 1997]. In this process, vertical as well as lateral gas escape may have a strong impact on the resulting viscosity profiles [*Collombet*, 2009]. It has been shown that degassing may be coupled with crystallization which, in turn, also affects magma viscosity [*Sparks*, 1997]. *Costa et al.* [2007a] consider a strong dependency of the viscosity on crystal content, with an increase in crystal content from 50 to 80 vol % leading to an increase in viscosity by a factor of 10^8. As a consequence of these shallow crystallization and degassing processes, a more viscous body, so-called plug, is typically emplaced at the upper part of the conduit. The presence of this degassed portion in the upper part of the conduit has been confirmed by petrological studies performed on explosive deposits at Soufrière Hills Volcano, Montserrat [*Burgisser et al.*, 2010]. The plug formation tends to reduce the magma flow rate and also induces a pressurization within the conduit. Changes in magma rheology modify the overall flow dynamics within the conduit and, consequently, the stress field within the surrounding crust, which might therefore induce precursor signals such as deformation or seismicity. Ground deformation related to conduit flow processes has been studied through analytic solutions [*Bonaccorso and Davis*, 1999; *Nishimura*, 2006, 2009] as well as numerical modelling [*Chadwick et al.*, 1988; *Beauducel et al.*, 2000; *Green et al.*, 2006; *Hautmann et al.*, 2009]. However, deformation of the conduit wall due to the magma flow was not taken into consideration and most of studies considered only one component of the stress field acting on the wall rocks, either shear stress [*Beauducel et al.*, 2000; *Green et al.*, 2006] or normal stress [*Hautmann et al.*, 2009]. Only few studies consider both components [*Chadwick et al.*, 1988; *Anderson et al.*, 2010]. However, in these studies, the two effects are evaluated independently despite their obvious link through flow motion equations [*Nishimura*, 2009].

Here, we consider the full coupling between the fluid flow and crustal deformation, taking into account the total stress field and the deformation of the conduit wall. We carry out numerical calculations in axial geometry to model the displacement field induced by a steady flow when a plug is emplaced at the top of the conduit. We perform a parametric study in order to quantify the deformation field induced by the increase of magma viscosity at the upper part of the conduit and give an estimation of the distance of detection of the induced signal. We then compare the magma flow rate and the surface tilt expected during plug growth within the conduit. We further discuss our results with regards to data recorded at the two most studied andesitic volcanoes, Soufrière Hills (Montserrat) and Mount St Helens (USA), and consider more realistic flow conditions as well as data acquisition geometry (including volcano topography).

2. Model

2.1. Description

Magma flow through a volcanic conduit embedded in the crust is modelled using a "Finite Element Method" (FEM) in axisymmetrical geometry (COMSOL software). The conduit is a vertical cylinder with radius (a_c) and length (L_c). The magma, considered as a Newtonian fluid, flows with steady state conditions due to an overpressure (P_c), which is an excess of pressure comparing to the lithostatic state, applied at the conduit bottom. This excess pressure is due to the presence of an overpressurized storage zone, which effect is not modeled in the present study. Our model is not time dependent and describes the departure induced by a given steady state magma flow within the conduit, from a reference state being a lithostatic state of stress within the surrounding rocks with an overpressurized reservoir not connected to the surface. It means that all the displacement and state of stress calculated are the one induced by the magma flow within the conduit. The surrounding crust is treated as a homogeneous elastic medium, characterized by its shear modulus (G) which will be variable and its Poisson's ratio (ν) which is fixed at 0.25 in all our study. Boundary conditions used for the host rock medium are the following (see Figure 1): (i) free displacements at the top boundary, which corresponds to the ground surface ; (ii) no vertical displacement at the bottom boundary and (iii) no radial displacement at the external lateral boundary. In order to neglect the boundary effects, the external lateral boundary of the elastic medium is located far away from the conduit (at a distance of 100 km). A full coupling of magma flow and crustal deformation is considered by applying the continuity of the stress field (Fig. 1), including normal as well as tangential components, at the conduit wall. Conduit wall deformation is calculated by an iterative process as described in Appendix A. Geometry, physical properties and boundary conditions applied in our model are shown in Figure 1a.

The steady state of fluid flow is solved from the Navier & Stokes equation. A complete parametric study is performed for an incompressible fluid with a constant density (ρ_m) equal to the surrounding crustal density, a viscosity function ($\mu(z)$) and characterized by a Poiseuille flow. We later consider in the discussion a compressible fluid associated to complex and realistic flow conditions. In the incompressible case, the component of the stress normal to the conduit wall is equal to the magma pressure. We first calculate perturbations of the reference state induced by the flow of a constant viscosity magma. This solution is then considered as our new state of reference. We then quantify displacements induced by the emplacement of a more viscous portion of the flow, so-called plug, at the top of the conduit with respect to the constant viscosity case.

To first order, the increase of viscosity is approximated by a step function (Fig. 1b) that is dependent on the conduit depth. The plug is characterized by two parameters: its viscosity (μ_p), with $\mu_p > \mu_m$ (μ_m being the viscosity of the magma column) and its length (h_p), with $h_p < \frac{1}{2}L_c$. For Poiseuille flow, with a constant viscosity, expressions for the stress field components at the conduit walls are simplified: (i) the normal stress is equivalent to the fluid pressure and varies linearly with depth, $\frac{dP}{dz} = cste$; (ii) the tangential stress or shear stress is a constant value, which only depends on the pressure gradient and the conduit radius, $\tau = (\frac{a_c}{2})(\frac{dP}{dz}) = cste$. In that case, and providing that the conduit deformation remains small (see Appendix A for conditions), we solve equations for the stress and displacement field within the elastic medium, applying the stress components corresponding to the fluid flow at the conduit wall. For magmas with constant viscosity (our reference case), the pressure gradient as well as the tangential stress applied at the conduit wall are constant $\tau_{ref} = \frac{a_c P_c}{2L_c}$ (the dashed curve on Fig. 1b). In this case, for a given Poisson's ratio, the surface displacements are a function of the conduit geometry (a_c, L_c), the overpressure at the bottom of the conduit (P_c) and the shear modulus (G) only. They do not depend on the viscosity value. For a plug model, the tangential stress is different from the reference case both at the upper part of the conduit (τ_{up}) and at the lower portion (τ_{low}) (solid curve in Fig. 1b). The increase of magma viscosity within the upper part induces an overpressure when compared to the reference case (of constant viscosity). This overpressure reaches a maximum value, denoted ΔP_p, at the base of the plug (Fig. 1b). At the plug bottom, the magma pressure, P_p, can be derived using the conservation of the volumetric flux along the conduit:

$$P_p = \frac{\mu_p h_p}{\mu_p h_p + \mu_m (L_c - h_p)} P_c \tag{1}$$

where P_c is the excess pressure at the conduit bottom. It follows that the overpressure (ΔP_p) can be expressed as a function of the viscosity contrast and the length ratio:

$$\Delta P_p = P_p - \frac{h_p}{L_c} P_c = \left(\frac{(\frac{\mu_p}{\mu_m})(\frac{h_p}{L_c})}{1 + \frac{h_p}{L_c}(\frac{\mu_p}{\mu_m} - 1)} - \frac{h_p}{L_c}\right) P_c \tag{2}$$

This overpressure is equal to zero when there is no viscosity contrast, $\mu_p = \mu_m$, and reaches the value $P_c(1 - \frac{h_p}{L_c})$ when the viscosity within the plug tends to infinity. For the plug case, the two magma viscosities, μ_m and μ_p, as well as the length of the plug, h_p, have an effect on the displacement. For a given Poisson's ratio and using the conduit length (L_c) as a length scale and the term $(\frac{P_c}{G} L_c)$ as a displacement scale, dimensionless solutions are only dependent on the following three dimensionless numbers: (i) the conduit aspect ratio

($\frac{a_c}{L_c}$), (ii) the length ratio between the plug and the total conduit ($\frac{h_p}{L_c}$), (iii) the viscosity ratio between the two magmas ($\frac{\mu_p}{\mu_m}$).

2.2. Main Limitations

Our model should be taken as a first attempt to link surface deformation as well as magma flow rate evolution to main characteristics of the magma properties evolution within its upper path to the Earth's surface. Here, we do not intent to solve the whole flow complexity but rather to couple a simple but coherent stress state with the deformation of the surrounding rocks. As a consequence our model contains a number of assumptions which have to be discussed. It is, however, noteworthy that many of these limitations could be reduced in further developments of the model.

The first assumption is the choice of a cylinder geometry to model the volcanic conduit. Magma, usually stored in a shallow reservoir, is connected to the surface through a crustal pathway. Dyke propagation is considered as the main mechanism which can initiate the pathway through the crust at deep level from the magma storage zone [*Lister and Kerr*, 1991; *Rubin*, 1995] and there are geological as well as geophysical evidences of the feeding of lava domes by dykes [*Mastin and Pollard*, 1988; *Nakada and Eichelberger*, 2004; *Roman et al.*, 2006]. However, for many andesitic volcanoes, such as Mt Usu (Japan), Soufrière Hills (Montserrat), Santiaguito (Guatemela) and Mt. St. Helens (USA), cylindrical conduits can develop during lava dome eruptions [*Yokoyama*, 1981; *Sparks and Young*, 2002; *Williams and Self*, 1983; *Swanson and Holcomb*, 1990]. Evidence of the existence of cylindrical conduit is supported by observations of the geometry of the crater vents and extruded bodies ("spine") during dome growth [*Sparks and Young*, 2002; *Iverson et al.*, 2006]. This particular shape is formed during explosive eruptions which frequently occurs before extrusive activity. One of the consequence is that the cylinder conduit is probably limited to the last hundred meters, but it can reach several kilometers in case of high fragmentation and large depressurization. The extension at depth of this cylindrical shape is still under debate. Some authors suggest a possible connection between a shallow cylindrical conduit and a deep dyke [*Costa et al.*, 2007b, a]. The effect of the pressurized dyke as well as a pressurized magma reservoir below the cylindrical conduit will act on magma flux and also on ground deformation on large time scale, over weeks to year. Here, we are interested in the short time scale deformation only occurring during rapid changes in magma flow dynamics at shallow level. In consequence, our model only focus on the shallow part of a mature magmatic system associated to cylindrical shapes, which has already been considered in many studies in relation with conduit flow [*Wylie et al.*, 1999; *Melnik and Sparks*, 1999; *Barmin et al.*, 2002; *Collier and Neuberg*, 2006; *Lensky et al.*, 2008; *Collombet*, 2009].

The second main assumption of our model is the choice of a Newtonian behaviour for the magma. Indeed, different processes, such as magma crystallization and cooling or high volatile contents may lead to a non-Newtonian behaviour, implying a dependence of the viscosity with the shear rate. The non-Newtonian behaviour is reached for high crystal-bearing magmas, containing more than 30-40% of crystals [*Pinkerton and Stevenson*, 1992; *Lejeune and Richet*, 1995]. This threshold can be reached in the case of Soufrière Hills [*Sparks et al.*, 2000] or Mt. St Helens [*Gardner et al.*, 1996] volcanoes if the andesitic magmas spend a significant duration in the conduit. Recent publications, such as [*Caricchi et al.*, 2007] show that, the magma behaviour is also highly dependent on the strain rate considered and for high values (above 10^{-4} s^{-1}) magma overall viscosity decreases with strain rates exhibiting non-Newtonian behaviour. In that case, the velocity profile should departs from the Poiseuille parabolic profile affecting values of the shear stress at the conduit wall. Considering Figure 3 from *Caricchi et al.* [2007] we can predict that the shear stress may decrease of approximately one order of magnitude comparing with the Newtonian case.

Another strong limitation of our model comes from the fact that thermal effects are not taken into account. However they could potentially favor non-Newtonian behaviour of the magma as well as affect stresses applied at the conduit wall. During ascent of hot magma in a cold crust, large thermal gradient can develop at the conduit wall. Mechanism of magma cooling or host rocks heating due to viscous effect can occur and the dominant effect depends on the flow conditions [*Costa et al.*, 2007c]. For example, a thermal boundary layer due to cooling effect should represent less than 0.5 m of the conduit radius and leads to a decrease of 100 to 200 K of temperature [*Collier and Neuberg*, 2006]. In opposite way, viscous heating effects can produce an increase of temperature at the wall and induce changes in the velocity profile of the flow, which evolves from parabolic (as we consider in our paper) to plug-like [*Costa and Macedonio*, 2005; *Costa et al.*, 2007c]. But these variations in temperature near the wall implies a melt viscosity change of one order of magnitude [*Hess and Dingwell*, 1996], which is much less than viscosity changes due to gas loss during magma ascent [*Sparks*, 1997]. In consequence, we believe that, despite this simplification, we capture the first order effect in our model.

3. Results

3.1. Surface Displacements

In this section, we explore a range of parameters for each dimensionless number to describe the influence of various parameters on the ground deformation. In each model, radial (U_r), vertical (U_z) displacements and tilt ($\frac{\delta U_z}{\delta r}$) at the surface are calculated. Radial and vertical displacements are positive when directed, respectively, outward and up from the conduit wall (see r,z direction in Fig. 1a). Tilts are negative when the surface is moving upward going toward the vent, which corresponds to a ground inflation. For all calculations, the Poisson's ratio value is 0.25. Results for the reference state (i.e. constant viscosity: $\frac{\mu_p}{\mu_m} = 1$) for three different conduit aspect ratios ($\frac{a_c}{L_c}$) are shown in Figure 3. The displacement trend is similar for various conduit aspect ratios except in the vicinity of the vent where differences are observed for radial distances less than 20% of the conduit length. The amplitude of the displacements and tilts is more important for larger values of $\frac{a_c}{L_c}$, corresponding to the largest or shortest conduits. This means, as previously shown by *Chadwick et al.* [1988], that a larger pressure is required to explain a given displacement when considering a smaller conduit radius. In Figure 3, we also show that displacements are both induced by the shear stress component and by the pressure. Both components induce displacements of the same order of amplitude. For radial displacements, shear stress has a strong influence in the near field (for $\frac{r}{L_c} < 0.5$) whereas pressure has more effect in the far field (for $\frac{r}{L_c} > 0.5$). For vertical displacements and tilts, pressure and shear stress induce opposite ground movement. Shear stress induces inflation whereas pressure induces deflation. However, the amplitude of the shear stress effect is larger, which results in a total displacement directed upward. In this case, neglecting the pressure component leads to an overestimate in the induced displacement field. For near field measurements, this overestimation is larger for a smaller conduit aspect ratio ($\frac{a_c}{L_c}$). For example, our model gives an overestimation, larger than 20% for the tilt at a distance of 500 m from the conduit, if pressure at the conduit wall is neglected, with the conditions taken by *Green et al.* [2006] to model tilt recorded at Montserrat volcano (i.e.: a shear stress of 0.5 MPa applied on the wall of a conduit with a 1000 m length and a 15 m radius and a Young's modulus fixed at 2 GPa). Thus, each stress component has an important effect on the total displacement field and none of them should be neglected in deformation models.

In case a viscous plug is present at the top of the conduit, displacements larger than those described above, for the constant viscosity case, are induced. We calculate surface tilts due to plug flow models exploring the range of 10^0-10^5 for the viscosity ratio ($\frac{\mu_p}{\mu_m}$) and 0-0.5 for the length ratio ($\frac{h_p}{L_c}$). Figure 4 shows the tilts calculated at a radial distance of 500 m from the conduit, for the tested parameter range, considering a conduit of 15 m radius and 5000 m length. Magma pressure at the conduit bottom (P_c) and the elastic shear modulus (G) of the crust are respectively fixed at 10 MPa and 0.8 GPa. Such values seem realistic for Soufrière Hills [*Green et al.*, 2006; *Costa et al.*, 2007b; *Voight et al.*, 1999]. Tilt calculation is relative to our reference case obtained with constant viscosity, such that it's value tends to zero when either h_p tends to zero or $\frac{\mu_p}{\mu_m}$ tends to 1. Figure 4a shows that the plug emplacement induces an inflation (negative tilt values). At 500 m from the conduit wall, tilt values reach more than 3 μrad for thin plugs characterized by a large viscosity contrast ($\frac{\mu_p}{\mu_m} > 10^{2.5}$ and $\frac{h_p}{L_c} < 0.05$). However the largest displacements are not always obtained with the thinnest plugs: for small viscosity ratios ($\frac{\mu_p}{\mu_m} < 10^3$), there exists a critical plug thickness, $h_{p(crit)}$, corresponding to a maximum of the induced tilt amplitude. For large viscosity ratios ($\frac{\mu_p}{\mu_m} > 10^3$), $h_{p(crit)}$ tends to zero: the tilt increases when the plug length decreases. In addition, for large viscosity ratio, tilt does not depend on the viscosity ratio, but is mainly a function of the plug length. The influence of each stress component on the ground displacements is also shown in Figure 4b and 4c. Even if the pressure acting along the conduit wall does not dominate the tilt signal, it has a strong influence inducing a ground deflation (positive tilt values). The effect is maximum, with an amplitude larger than 1 μrad, for intermediate length ratios (between 0.1 and 0.3). In most cases, except for the thinnest plugs, neglecting the pressure effect leads to overestimate the induced tilt, which means that the tangential stress component will be underestimated when interpreting an observed signal.

3.2. Detection of Ground Deformation

We have showed that an increase of magma viscosity occurring at the top of a conduit, increases tilts at the ground surface. In order to guide the choice for in-situ instrument types and locations, it seems important to quantify the maximal distance from the volcanic vent, where this signal can be detected. We estimate this critical distance, hereafter called ”detection distance” using a threshold value of detection for each component of the displacement. Horizontal and vertical ground movements can be detected by GPS receivers. The theoretical precision of the instrumentation used in volcanology is around 5 mm and 10 mm respectively for the horizontal and vertical displacement (http://www.igage.com/GPSaccy/index.html). However, field measurements can be perturbed by the atmospheric component or local perturbations of the instrumented site. We thus assume in our study that only millimetric changes for the radial displacements and centimetric changes for the vertical displacements will be detected. On the other hand, a more accurate method to detect ground motion is to measure the tilt of the volcano surface. According to the tiltmeters used, ground deformation less than 1 μrad can be detected (http://www.carboceramics.com/Tiltmeters-Clinometers), one microradian corresponding to a vertical variation of one millimeter over a distance of one kilometer. This type of measurement is difficult to set up because instruments are highly sensitive to changes in temperature or atmospheric pressure. In order to minimize the influence of these external effects on recorded measurements, tiltmeters are often placed in boreholes, several centimeters beneath the surface. Here, we choose an upper value for our detection threshold and we consider that only tilt variations larger than 1 μrad are detected.

We use the same model parameters as in Figure 4 ($G = 0.8$ GPa, $\nu = 0.25$, $P_c = 10$ MPa, $L_c = 5000$ m and $a_c = 15$ m) and threshold values of 1 mm and 1 cm respectively for the radial and the vertical displacements, and 1 μrad for the tilt. We find that: (i) radial displacement is never detectable for plugs representing more than 20% of the total conduit, but it can be observed over 1 km for plugs with length ratio less than 10% and viscosity contrast more than 10^2 (see figure 5a). (ii) vertical displacement can never be detected, except a few meters from the conduit for the thinnest plugs (see figure 5b). (iii) tilt can be detected for a few hundred meters depending on the plug characteristics as detailed in Figure 6c. Tiltmeters or GPS located at a few hundred meters from the conduit are thus appropriate to detect the ground deformation, respectively tilt or radial displacement, induced by plug emplacement within the upper part of a volcanic conduit. As previously explained, the amplitude of the displacements is not only dependent on the viscosity ratio ($\frac{\mu_p}{\mu_m}$) and length ratio ($\frac{h_p}{L_c}$) but is also function of the balance between the reservoir overpressure and the host rocks elastic properties, $\frac{P_c}{G}$, as well as the conduit aspect ratio ($\frac{a_c}{L_c}$). Figure 6 shows the effect of these two parameters on the detection distance. The case c) is calculated for a radius a_c equal to 15 m and a shear modulus G equal to 0.8 GPa, values previously used. The case a) provides the detection distance for a larger radius (a_c), the case d) for a larger shear modulus (G) and the case b) when both parameters are increased. As expected, an increase of the conduit radius or a decrease of the host rocks shear modulus, tends to increase the detection distance for tilt signal. During the extrusive phase, the detection of ground deformation caused by plug emplacement will be much easier in the case of andesitic volcanoes with a large conduit embedded in soft host rocks.

3.3. Flow Rate Versus Tilt Signal During Plug Evolution

The formation of a viscous plug at the top of the volcanic conduit induces a decrease of magma flow. The flow rate for a plug model can be expressed as a function of the reference flow rate, Q_{ref}, of the "constant viscosity" case:

$$Q = \left(\frac{1}{1 + \frac{h_p}{L_c}\left(\frac{\mu_p}{\mu_m} - 1\right)}\right) Q_{ref} \tag{3}$$

In the previous section, we showed that plug emplacement also induces ground motion signals large enough to be detected under certain conditions. During the extrusive phases of andesitic volcanoes, a plug may form in the upper portion of the conduit and evolve through time due to continuous degassing as well as cooling and crystallization processes. Plug evolution can proceed either through an increase of its viscosity or its size. In nature, both cases are probably mixed, but here we choose to compare the relative evolution of tilt and flow rates observed at the surface as a consequence of these two end-members (Figure 7).

For a given plug length, an increase of plug viscosity reduces, as expected, the magma flow rate produced at the surface (Fig. 7b, left panel). As a consequence of this flow rate decrease, the amount of time required to entirely extrudes the plug considered (thickness h_p and viscosity μ_p), increases (Fig. 7c, left panel). This duration corresponds to the expected duration of the deflation induced by the plug extrusion. Whatever the value of $\frac{h_p}{L_c}$, the flow rate falls below 5% of its reference value for a viscosity contrast larger than 10^3. This increase of viscosity induces a ground inflation: the tilt amplitude first increases with the viscosity contrast before reaching a constant and maximum value (Fig. 7a, left panel). The threshold value of viscosity at which the maximum of tilt amplitude is reached, depends on the plug size, with larger values for thinner plugs. For plugs that are more viscous than the threshold value, the tilt amplitude remains constant and the magma flow rate is close to zero. Thus, if a high contrast of viscosity already exists between the plug and the magma column, the evolution of the plug viscosity can not be detected from the surface displacement measurements.

The other end-member behaviour is the one induced by a thickening plug of constant viscosity. Once again due to plug evolution, the magma flow rate decreases (Fig. 7b, right panel) and the extrusion duration consequently increases (Fig. 7c, right panel). However for small viscosity contrasts, the flow rate reduction remains small. For the induced tilt (Fig. 7a, right panel), the behaviour is different than in the previous case: we observe a rapid ground inflation (upward displacement when going towards the crater), until the plug reaches its critical thickness, $h_{p(crit)}$, as previously defined. Once the plug thickness is larger than this critical value, the tilt amplitude decreases together with the flow rate. For a large viscosity contrast, the critical thickness tends to zero, and the first phase can not be distinguished. This result is related to the fact that the maximum amplitude of the surface tilts is not always obtained for the thinnest plugs but for a critical plug size, which depends on the viscosity contrast. For plugs larger than the critical thickness, the decrease trend of the tilt amplitude is mainly controlled by the variation of the pressurization level (h_p) rather than its value (ΔP_p). Indeed, an increase of the plug length corresponds to an increase of the depth of the maximal pressurization within the conduit.

To summarize, in the early stage of plug emplacement (a small viscosity contrast and a thin thickness), the resulting increase of overpressure due to the plug, ΔP_p, induces an inflation, while the magma flow rate is reduced. Depending on the preponderant effect during plug growth, either in the thickness or in the viscosity contrast evolution, an increase or a decrease of tilt amplitude might occur afterward. The joint interpretation of the flow rate and ground motion evolution through time, using this kind of model, can thus provide useful constrains on magma viscosity profiles within the conduit. Tracking the evolution of magma physical properties through time is essential to explain drastic and sudden changes of magmatic activity observed at andesitic volcanoes.

4. Discussion

4.1. Effect of Conduit Flow Versus Other Deformation Sources

In this study, we have modelled ground motion due to magma conduit flow considering no pressure changes within the magma reservoir and no magma accumulation at the surface. It is obvious, however, that flow dynamics changes occurring within the conduit are not the only source of deformation on andesitic strato-volcanoes. Pressure changes within a shallow magma reservoir [*Mogi*, 1958] and surface load variations due to dome growth/collapse can also induce ground motion [*Beauducel et al.*, 2000]. Figure 8 allows a comparison of the relative amplitude of these various phenomena. It shows displacements induced by (i) surface pressure change of 1 MPa related to the emplacement/removal of a lava dome (1 MPa corresponding to a height change of 60 m of a material with a density of 1700 kg.m^{-3}), (ii) an overpressure variation of 1 MPa occurring within a magma reservoir and (iii) the emplacement of a plug in the upper part of the conduit. All the parameters taken for these models are detailed in the caption of the Figure 8. In the far field, at distances greater than 0.2 L_c from the volcanic vent, magma pressure changes or dome height variations induce larger displacements at the Earth's surface than the magma conduit flow. Emplacement of a plug at the top of the conduit might induce larger amplitudes than magma reservoir or lava dome processes, in radial displacements as well as in tilt signal, only in the immediate vicinity of the vent.

To conclude, with the context of an incompressible magma, ground motion induced by magma viscosity increases at the top of the volcanic conduit will be detectable only if: (i) instruments are located in the near field, few hundred meters from the volcanic vent ; (ii) plugs have reduced size and high viscosity contrast compared to the magma column ; (iii) other processes, such as magma reservoir pressure changes or lava dome growth/collapse, do not dominate the deformation signal. *Melnik and Sparks* [2005] proposed a transient model of magma flow in an open volcanic conduit including gas exsolution and escape, bubble growth as well as crystallization effects. They show that the system can fluctuate between two stable states, one being characterised by a high flow rate of less viscous magma and the other by a low flow rate of more viscous magma. Considering the given viscosity profiles and reservoir overpressures, we have quantified the induced displacements when the system goes from one regime to the other. Deformation at the surface is almost entirely due to the pressure changes occurring within the reservoir, the viscosity profile changes occurring within the conduit having a smaller effect. However the model proposed by *Melnik and Sparks* [2005] cannot simultaneously explain cycles occurring on a period of several years or several weeks. Short time-scales cycles have been explained by models with a constant reservoir pressure [*Costa et al.*, 2007b], which justifies our choice to quantify the displacement field induced by magma flow condition within the conduit in case there is no magma reservoir pressure change.

Conversely, the fact that conduit effects might dominate the deformation signal in the immediate vicinity of the vent, implies the necessity to have some distant instruments in order to monitor magma pressure changes within storage zones.

4.2. Influence of Topography

In all previous calculations, the volcano surface is modelled as a flat surface, but andesitic strato-volcanoes are characterized by significant topography with slopes up to 35°. Because topography can have an effect on ground deformation results [*Cayol and Cornet*, 1998], we calculated tilts induced by plug emplacement with an upper surface corresponding, in the first approximation (a linear trend), to Montserrat topography. Including this topography, we obtained the same conclusions as for a flat topography,

4.3. Influence of Viscosity Profile

At Soufrière Hills Volcano (Montserrat), tilt cycles were recorded at 600-700 m from the crater vent, first in December 1996 with an amplitude of 1-2 μrad and a period of 6-8 h, and few months after, from April to May 1997, with an amplitude between 10 and 25 μrad and a period of 12-18 h [*Voight et al.*, 1998]. The cyclic behaviour of the surface deformation, with a deflation phase more rapid than the inflation one, is also correlated with cycles in seismic activity and gas emissions of SO_2 [*Watson et al.*, 2000]. At Mt St Helens, variations of the tilt amplitude were also measured during the active period between the years 2004 and 2008 by *Anderson et al.* [2010]. Tiltmeters, located within the crater and close the dome (around 150-250 m from the vent), recorded many cyclic tilt events characterized by a duration from minutes to hours and a mean amplitude close to 1 μrad. The pattern of the cycle begin with, a rapid inflation (outward tilt) followed by a gradual subsidence (inward tilt). Here, we compare the amplitude of tilt recorded at Montserrat and Mt St Helens with those obtained by our plug models (Fig. 9b). Assuming a value of 0.8 GPa for the shear modulus, 0.25 for the Poisson's ratio and 10 MPa for the magma reservoir overpressure, a high viscous plug emplaced in the upper part of the conduit can produce the amplitude of tilt cycles recorded at both volcanoes. At Mt St Helens, surface tilt induced by a plug occupying 25 % of the conduit fits the data collected during the period July 1996-January 1997. In the same way, at Soufrière Hills, a plug emplaced in the upper 10 % of the conduit can also explain the tilt data recorded during December 1996. However, our plug models cannot produce the large tilt amplitude of 10-25 μrad measured during the April-May 1997 at Montserrat. In our model, we always assumed that viscosity increase at the top of the conduit follows a step function and we consider that the magma density is constant over the conduit. But, this viscosity profile is simplified and magma density also evolves with depth. To overcome this simplification, we also calculated tilt induced by other flow models considering realistic viscosity profiles, and compare to results previously obtained with our plug model. The first one is taken from *Sparks* [1997] and corresponds to the model 3 presented in the paper as a case "where a lava dome up to 100 m thick is being fed from a conduit and the gas is lost during ascent for magma that just remains gas-saturated at the local pressure". In this model, the viscosity profile is expressed as a power law of the depth and increases progressively from the bottom of the conduit to the surface. We solved the Navier-Stokes equations for an incompressible magma using this viscosity profile and applied the resulting stress at the conduit wall in order to calculate the displacement field. The other viscosity profile considered is obtained from *Collombet* [2009]. We used the stationary solution for flow conditions described by *Collombet* [2009] and applied the resulting stress at the conduit wall. In comparison with the previous models that only consider vertical gas escape, it also takes into account the lateral gas loss due to the permeability of the conduit wall. This model is suitable to model effusive activity, such as dome construction of andesitic strato-volcanoes because it allows to consider realistic initial volatiles content and to reproduce quite precisely the vesicularity of the degassed magma, which is consistent with the observations made on real domes. With this model, a large viscosity change occurs only in the upper few hundred metres of the conduit, which induces large stresses at the conduit wall close to the surface (Fig. 9a). The particularity of this last model is that, for shallow depths (above 750 m depth), magma overpressure in the conduit reaches larger values than those applied at the conduit bottom, due to magma compressibility effects. This large pressure gradient as well as the high shear stress at shallow levels of the conduit produced a tilt amplitude one order of magnitude larger than the two other models (Fig. 9b). Assuming a value of 0.8 GPa for the shear modulus and 10 MPa for the magma reservoir overpressure, the model obtained from *Collombet* [2009], taking into account a compressible magma and the vertical as well as the lateral degassing, seems to better explain the amplitude of the tilt inflation measured in Soufrière Hills Volcano during the April-May period.

4.4. Origin of Cyclic Deformation

The formation of a viscous plug in the shallow part reduces the magma flow rate and builds up large overpressures in the last few hundred metres, which may cause the tilt inflation observed at the surface. Plug formation is well explained by the magma viscosity increase as a consequence of exsolution, gas loss, cooling and crystallization processes. In order to account for the cyclic behaviour, an explanation for the following depressurisation is required. In most cases, the mechanism invoked is a stick-slip transition. Above a threshold criterion, rapid plug motion occurs because the magma starts to slip along the conduit walls, the speed of slip being a function of the wall friction. The plug is extruded and the magma pressure is released, causing the return to the initial state without the plug. The threshold criterion used is either a given overpressure within the magma below the plug [*Lensky et al.*, 2008] or the condition for brittle failure of the magma [*Collier and Neuberg*, 2006]. The onset of brittle failure has been identified to occur when the product of the melt viscosity and the shear strain rate is larger than the shear strength of the melt (σ_s) [*Webb and Dingwell*, 1990], values being estimated between 10^7 and 10^8 Pa for pure glass [*Tuffen et al.*, 2003; *Tuffen and Dingwell*, 2005].

In our plug flow model, this criterion is equivalent to $\tau_{up} = \dfrac{a_c}{2}\dfrac{P_p}{h_p} > \sigma_s$ and thus only depends on the conduit radius, the plug thickness and the pressure at the plug bottom. Largest shear stress is obtained for the most viscous and the thinnest plugs. From a value of magma shear strength of 10^7 Pa and classic values for Montserrat case of 15 m and 10 MPa respectively for the conduit radius (a_c) and the bottom pressure (P_c), we deduce than the plug length (h_p) must be less than 7.5 m to reach the magma failure. *Burgisser et al.* [2011] suggest a thickness of a few tens of meters or even less for the dome plug, such that a thin plug might be possible. If we know consider a plug size of 50 m, a bottom overpressure larger than the 66.7 MPa is required for a 15 m radius conduit. In the case of a more realistic overpressure of 10 MPa, the brittle failure of the magma is obtained if the conduit radius is larger than 100 m. Based on these results, conditions required to cause magma failure remain unlikely, such that we used a no-slip condition at the conduit wall. However, there is some experimental as well as textural evidence of magma brittle failure in the upper portion of volcanic conduits [*Lavallée et al.*, 2008; *Tuffen et al.*, 2008]. The value of shear strength we used might be overestimated for real magma and our Newtonian flow model does not well describe the stress gradient close to the conduit where the deformation is expected to be very localised.

Another way to account for plug removal is to consider a modification of permeability at the conduit wall as proposed by *Edmonds et al.* [2003]. For example, *Taisne and Jaupart* [2008] have shown that the loading of the crater floor by the dome acts to prevent gas leakage from magma by closing fractures around the volcanic conduit. A permeability decrease would prevent lateral degassing and might reduce the plug either by decreasing its viscosity contrast or its length. This is consistent with the fact that, as at Soufrière Hills (Montserrat), a decrease in SO_2 emission rate was observed prior to the start of magma ascent, after a pause in dome growth [*Edmonds et al.*, 2003]. In this case, the evolution of the plug, from one state of equilibrium to another, requires more time than in the case of slip by rupture. Based on the flow rate and plug geometry, we can calculate the amount of time required for the entire extrusion of the plug. This value is represented in Figure 7c and provides a lower bound for the duration of the deflation induced by the plug removal. In case of the calculation based on the viscosity profile taken from *Sparks* [1997], this duration is close to 12 hours whereas for the calculation based on the model developed by *Collombet* [2009] this duration is close to one hour, such that both models are consistent with the cycle duration recorded in 1997 at Montserrat Volcano.

4.5. Origin of Tilt Reversals Before Eruptions

Reversals of ground tilt direction have been documented before eruptions. *Chadwick et al.* [1988] showed that before extrusions occurring at Mount St Helens from May 1981 to August 1982, outward tilting was observed during several weeks, accelerated sharply and then abruptly changed direction to inward tilting, minutes to hours before eruptive activity began. Such a phenomenon could be linked to a variation of magma pressure within a shallow reservoir. It would be consistent with a pressure increase due to replenishment or degassing occurring weeks before the eruptive event and followed by a pressure decrease as a response to magma discharge within a propagating dyke forming intrusion. However, in this case, the source of the ground deformation is likely to be located within the conduit as proposed by *Chadwick et al.* [1988]. A possible explanation might come from the evolution of the plug within the volcanic conduit. As shown in Figure 10, considering the plugged conduit as the reference state (high value of $\frac{h_p}{L_c}$), the decrease of the plug thickness induces first an increase of the vertical displacement and tilt, correlated to a relative constant flow rate. These displacements correspond to a ground inflation with the slopes of the volcano tilting away from the volcanic vent. The inflation is followed by a decrease of ground displacements, which indicates a phase of rapid deflation. During this subsidence, the magma flow rate rapidly increases to reach its maximal value when the plug is totally removed ($\frac{h_p}{L_c} = 0$). Because the ground movement has changed in direction, the surface of the volcano now tilts towards the vent. As a result, the process of thickness variation development of a viscous plug in a volcanic conduit can be a possible origin for the tilt reversal observed before an eruption at andesitic volcanoes, such as Mount St Helens.

5. Conclusions

We estimated ground deformation induced at a volcano surface by magma viscosity changes occurring in the upper portion of the conduit. Calculations were performed considering a simplified viscosity profile for the magma, the viscosity taking two different values: a higher value within the plug and a lower value within the magma column itself, below. This model provides a good estimation of ground displacement, not very different, in amplitude, from the one produced by more realistic models with power-law profiles of viscosity. Plug emplacement results in a decrease of the magma discharge rate together with a rise of the shear stress levels along the conduit walls, which is considered to be the main source of displacements at the surface. However, even if it is most often dominant, the shear stress effect is not the only effect of importance: the conduit is also pressurized all along the conduit, the maximum of pressurization occurring at the plug bottom. This pressurization has a significant effect on surface deformation and should not be neglected. For the case of Soufrière Hills Volcano at Montserrat, neglecting the pressure effects leads to an overestimation, larger than 20 percent, of the tilt measured at 500 m from the crater. Plug growth always results in an overall decreasing magma flow rate, whereas it may either induce an increase or a decrease of the outward tilt, depending on the magnitude and the depth of the pressurization level. Joint interpretation of magma flow rates and surface displacements can bring strong constrain on the plug thickness and viscosity evolution. In absence of dome load or magma reservoir pressure variations, radial displacements or tilt signals caused by plug emplacement might be detected only a few hundred metres from the crater vent, according to the size and the viscosity of the plug as well as the size of the conduit and the mechanical properties of the host rocks. This conclusion becomes even more restrictive in case the dome geometry evolves by collapse or rapid magma emplacement or in case magma reservoir pressure variations occur. Then a plug emplacement might dominates the tilt as well as radial displacements only in the immediate vicinity of the conduit (less than 100 m). The estimated distance of detection should be taken into consideration when deciding for the type and the location of geodetic instrumentation at andesitic volcanoes. Or simplified model of plug emplacement can explain the amplitude around 1 μrad of tilt signals recorded at Mt St Helens or Soufrière Hills Volcano at Montserrat in December 96. However, in order to explain the amplitude recorded, at Soufrière Hills, from May to August 2007, when the tilt reached more than 10 μrad, we need to consider compressible magma characterized by a more realistic viscosity profile resulting from vertical as well as lateral degassing.

Appendix A: Fluid-Solid Interaction

In our study, we treat the full coupling between the fluid and the elastic solid by an iterative process. At each step, we solve for the fluid flow, apply the resulting stress components at the conduit wall, and then we calculate the displacements at the conduit walls and modify, in consequence, the geometry of the fluid domain boundaries. We iterate this process chain until convergence occurs. Usually convergence is immediate because the radial displacements of the conduit wall is small. This radial displacement can be approximated analytically. Neglecting the tangential stress effects and considering that the pressure gradient with depth remains small, we can use the solution of an infinite pressurised pipe with an axial geometry to estimate, to a first approximation, the radial displacement of the conduit wall. It gives $U_r = \frac{1}{2}(\frac{P_c}{G})a_c$ [*Landau and Lifshitz*, 1975; *Love*, 1987], where P_c is the overpressure at the conduit bottom, G the shear modulus of host rocks and a_c the conduit radius. In volcanic conduits, the magma overpressure does not exceed values of 20 MPa [*Melnik and Sparks*, 1999] and the shear modulus is around 1-10 GPa [*Costa et al.*, 2007b; *Voight et al.*, 1999; *Barmin et al.*, 2002]. So, the amplitude, therefore, of the radial displacement (U_r) at the conduit wall remains smaller than 1% of the conduit radius. For a 10 metre radius, the expected maximal wall displacement will be only 10 centimeters. We quantified, in our plug model, the effect of this wall deformation on the displacement field at the surface. First, wall deformation has a larger effect for a low shear modulus (G) and a large overpressure (P_c). Secondly, from a shear modulus of 0.4 GPa and a magma overpressure of 10 MPa, the amplitude of the surface displacements is only 5% larger when we take into account the conduit wall deformation compared with the rigid conduit case. In many volcanic contexts, the effect of conduit wall deformation will not affect significantly the surface displacements and can thus be neglected to a first approximation.

Appendix B: Model validation

Numerical solutions have been compared to existing analytic solutions in order to validate our model. First we used our numerical simulation to estimate the radial displacement induced, at the surface, by a pressurized pipe, with a uniform pressure P_c, embedded in an elastic half-space. Results were compared with the solution given by the following analytic expression [*Love*, 1987]: $U_r = \frac{a_c^2 P_c}{2rG}$, where r is the radial distance. Secondly, the tilt induced, at the surface, by a constant shear stress applied along the conduit wall, was numerically estimated and compared to the analytic expression provided by *Anderson et al.* [2010], which corresponds to an approximate solution derived from the integration of the Green's functions of a vertical point force. The comparison between numerical results and analytic solutions as well as the estimated error are shown in Figure 11. The error is the relative difference in percent between the analytic calculation and our numerical results. This figure shows that the error is the largest at the smallest distance from the conduit. However, for a distance larger than 50 meters, the error remains smaller than 2 % for the pressurised pipe (case a) and close to 0 for the conduit with an applied shear stress (case b).

Acknowledgments. This study was supported by IRD. We are very grateful for helpful reviews from the Associate Editor M. Ryan, A. Costa, V. Cayol and an anonymous reviewer.

References

Anderson, K., M. Lisowski, and P. Segall, Cyclic ground tilt associated with the 2004-2008 eruption of mount St. Helens, *J. Geophys. Res.*, *115*, 2010.

Barmin, A., O. Melnik, and R. Sparks, Periodic behavior in lava dome eruptions, *Earth Planet. Sci. Lett.*, *199*, 173–184, 2002.

Beauducel, F., F.-H. Cornet, E. Suhanto, T. Duquesnoy, and M. Kasser, Constraints on magma flux from displacements data at Merapi volcano, Java, Indonesia, *J. Geophys. Res.*, *105*, 8193–8203, 2000.

Bonaccorso, A., and P. Davis, Models of ground deformation from vertical conduits with application to eruptions of Mount St. Helens and Mount Etna, *J. Geophys. Res.*, *104*, 10,531–10,542, 1999.

Burgisser, A., S. Poussineau, L. Arbaret, T. Druitt, T. Giachetti, and J.-L. Bourdier, Pre-explosive conduit conditions of the 1997 Vulcanian explosions at Soufrière Hills Volcano, Montserrat: I. Pressure and vesicularity distributions, *J. Volcanol. Geotherm. Res.*, *194*, 27–41, 2010.

Burgisser, A., L. Arbaret, T. Druitt, and T. Giachetti, Pre-explosive conduit conditions of the 1997 Vulcanian explosions at Soufrière Hills Volcano, Montserrat: II. Overpressure and depth distributions, *J. Volcanol. Geotherm. Res.*, *199*, 193–205, 2011.

Caricchi, L., L. Burlini, P. Ulmer, T. Gerya, M. Vassalli, and P. Papale, Non-Newtonian rheology of crystal-bearing magmas and implications for magma ascent dynamics, *Earth Planet. Sci. Lett.*, *264*, 402–419, 2007.

Cayol, V., and F. Cornet, Effects of topography on the interpretation of the deformation field of prominent volcanoes - Application to Etna, *Geophys. Res. Letters*, *25*, 1979–1982, 1998.

Chadwick, W., R. Archuleta, and D. Swanson, The Mechanics of Ground Deformation Precursory to Dome-Building Extrusions at Mount St. Helens 1981-1982, *J. Geophys. Res.*, *93*, 4351–4366, 1988.

Collier, L., and J. Neuberg, Incorporating seismic observations into 2D conduit flow modeling, *J. Volcanol. Geotherm. Res.*, *152*, 331–346, 2006.

Collombet, M., Two-dimensional gas loss for silicic magma flows: toward more realistic numerical models, *Geophys. J. Int.*, *177*, 309–318, 2009.

Costa, A., and G. Macedonio, Viscous heating in fluids with temperature-dependent viscosity: Triggering of secondary flows, *J. Fluid Mech.*, *540*, 21–38, 2005.

Costa, A., O. Melnik, and R. Sparks, Controls of conduit geometry and wallrock elasticity on lava dome eruptions, *EPSL*, *260*, 137–151, 2007a.

Costa, A., O. Melnik, R. Sparks, and B. Voight, Control of magma flow in dykes on cyclic lava dome extrusion, *Geophys. Res. Letters*, *34*, L02,303, 2007b.

Costa, A., O. Melnik, and E. Vedeneeva, Thermal effects during magma ascent in conduits, *J. Geophys. Res.*, *112*, 2007c.

Denlinger, R., and R. Hoblitt, Cyclic eruptive behavior of silicic volcanoes, *Geology*, *27*, 459–462, 1999.

Edmonds, M., C. Oppenheimer, D. Pyle, R. Herd, and G. Thompson, SO_2 emissions from Soufrière Hills Volcano and their relationship to conduit permeability, hydrothermal interaction and degassing regime, *J. Volcanol. Geotherm. Res.*, *124*, 23–43, 2003.

Gardner, J., R. Thomas, C. Jaupart, and S. Tait, Fragmentation of magma during Plinian volcanic eruptions, *Bull. Volcanol.*, *58*, 144–162, 1996.

Green, D., J. Neuberg, and V. Cayol, Shear stress along the conduit wall as a plausible source of tilt at Soufrière Hills volcano, Montserrat, *Geophys. Res. Letters*, *33*, L10,306, 2006.

Harris, A., W. Rose, and L. Flynn, Temporal trends in lava dome extrusion at Santiaguito 1922-2000, *65*, 77–89, 2002.

Hautmann, S., J. Gottsmann, R. Sparks, A. Costa, O. Melnik, and B. Voight, Modelling ground deformation caused by oscillating overpressure in a dyke conduit at Soufrière Hills Volcano, Montserrat, *Tectonophysics*, *471*, 87–95, 2009.

Hess, K.-U., and D. Dingwell, Viscosities of hydrous leucogranitic melts: A non-Arrhenian model, *American Mineralogist*, *81*, 1297–1300, 1996.

Iverson, R., et al., Dynamics of seismogenic volcanic extrusion at Mount St Helens in 2004-05, *Nature*, *444*, 439–443, 2006.

Landau, L., and E. Lifshitz, *Theory of elasticity*, 2nd ed. ed., Pergamon, Tarrytown, N.Y., 1975.

Lavallée, Y., P. Meredith, D. Dingwell, K.-U. Hess, J. Wassermann, B. Cordonnier, A. Gerik, and J. Kruhl, Seismogenic lavas and explosive eruption forecasting, *Nature*, *453*, 507–509, 2008.

Lejeune, A., and P. Richet, Rheology of crystal-bearing silicate melts: An experimental study at high viscosities, *J. Geophys. Res.*, *100*, 4215–4229, 1995.

Lensky, N., R. Sparks, O. Navon, and V. Lyakhovsky, Cyclic activity at Soufrière Hills Volcano, Montserrat: degassing-induced pressurization and stick-slip extrusion, in *Fluid Motions in Volcanic Conduits: A Source of Seismic and Acoustic Signals*, vol. 307, Geological Society ed., pp. 169–188, Lane, S.J. & Gilbert, J.S., London, 2008.

Lister, J., and R. Kerr, Fluid-Mechanical models of crack propagation and their application to magma transport in dikes, *J. Geophys. Res.*, *96*, 10,049–10,077, 1991, archimede.

Llewellin, E., and M. Manga, Bubble suspension rheology and implications for conduit flow, *J. Volcanol. Geotherm. Res.*, *143*, 205–217, 2005.

Love, A., *A Treatise on the mathematical theory of elasticity*, Dover Classics of Sciences and Mathematics, 4th ed., Dover, 1987.

Mastin, G., and D. Pollard, Surface Deformation and Shallow Dike Intrusion Processes at Inyo Craters, Long Valley, California, *J. Geophys. Res.*, *93*, 13,221–13,235, 1988.

Melnik, O., and R. Sparks, Nonlinear dynamics of lava dome extrusion, *Nature*, *402*, 37–41, 1999.

Melnik, O., and R. Sparks, Controls on conduit magma flow dynamics during lava dome building eruptions, *J. Geophys. Res.*, *110*, 2005.

Mogi, K., Relations between the eruptions of various volcanoes and the deformation of the ground surfaces around them, *Bull. Earthquake Res. Inst., Univ. Tokyo*, *36*, 99–134, 1958, analytic.

Nakada, S., and J. Eichelberger, Looking into a volcano: drilling Unzen, *Geotimes*, *49*, 14–17, 2004.

Nakada, S., H. Shimizu, and K. Ohta, Overview of the 1990-1995 eruption at Unzen Volcano, *J. Volcanol. Geotherm. Res.*, *89*, 1–22, 1999.

Nishimura, T., Ground deformation due to magma ascent with and without degassing, *Geophys. Res. Letters*, *33*, L23,309, 2006.

Nishimura, T., Ground deformation caused by magma ascent in an open conduit, *J. Volcanol. Geotherm. Res.*, *187*, 178–192, 2009.

Pinkerton, H., and R. Stevenson, Methods of determining the rheological properties of magmas at sub-liquidus temperatures, *J. Volcanol. Geotherm. Res.*, *53*, 47–66, 1992.

Roman, D., J. Neuberg, and R. Luckett, Assessing the likelihood of volcanic eruption through analysis of volcanotectonic earthquake fault-plane solutions, *Earth Planet. Sci. Lett.*, *248*, 244–252, 2006.

Rubin, A., Propagation of magma-filled cracks, *Ann. Rev. Earth Planet. Sci.*, *23*, 287–336, 1995.

Shaw, H., Obsidian-H20 Viscosities at 1000 and 2000 Bars in the Temperature Range 700° to 900°C, *J. Geophys. Res.*, *68*, 6337–6343, 1963.

Sparks, R., Causes and consequences of pressurisation in lava dome eruptions, *Earth Planet. Sci. Lett.*, *150*, 177–189, 1997.

Sparks, R., and S. Young, The eruption of Soufrière Hills volcano, Montserrat (1995-1999): overview of scientific results, in *The eruption of the Soufrière Hills Volcano, Montserrat from 1995 to 1999*, edited by T. Druitt and B. Kokelaar, pp. 45–69, Geological Society, 2002.

Sparks, R., M. Murphy, A. Lejeune, R. Watts, J. Barclay, and S. Young, Control on the emplacement of the andesite lava dome of the Soufrière Hills Volcano, Montserrat by degassing-induced crystallization, *Terra Nova*, *12*, 14–20, 2000.

Swanson, D., and R. Holcomb, Regularities in growth of the Mount St. Helens dacite dome 1980-1986, in *Lava Flows and Domes: Emplacement and Mechanisms and Hazards Implications*, Springer ed., pp. 3–24, J.H. Fink, New York, 1990.

Taisne, B., and C. Jaupart, Magma Degassing and Intermittent Lava Dome Growth, *Geophys. Res. Letters*, *35*, 2008.

Tuffen, H., and D. Dingwell, Fault textures in volcanic conduits: evidence for seimic trigger mechanisms during silicic eruptions, *Bull. Volcanol.*, *67*, 370–387, 2005.

Tuffen, H., D. Dingwell, and H. Pinkerton, Repeated fracture and healing of silicic magma generate flow banding and earthquakes?, *Geology*, *31*, 1089–1092, 2003.

Tuffen, H., R. Smith, and R. Sammonds, Evidence for seismogenic fracture of silicic magma, *Nature*, *453*, 511–513, 2008.

Voight, B., R. Hoblitt, A. Clarke, A. Lockhart, A. Miller, L. Lynch, and J. McMahon, Remarkable cyclic ground deformation monitored in real-time on Montserrat, and its use in eruption forecasting, *Geophys. Res. Letters*, *25*, 3405–3408, 1998.

Voight, B., E. Constantine, S. Siswowidjoyo, and R. Torley, Historical eruptions of Merapi Volcano, central Java, Indonesia, 1768-1998, *J. Volcanol. Geotherm. Res.*, *100*, 69–138, 2000.

Voight, B., et al., Magma Flow Instability and Cyclic Activity at Soufriere Hills Volcano, Montserrat, British West Indies, *Science*, *283*, 1999.

Voight, B., et al., Unprecedented pressure increase in deep magma reservoir triggered by lava-dome collapse, *Geophys. Res. Letters*, *33*, 2006.

Watson, I., et al., The relationship between degassing and ground deformation at Soufriere Hills Volcano, Montserrat, *J. Volcanol. Geotherm. Res.*, *98*, 117–126, 2000.

Webb, S., and D. Dingwell, Non-Newtonian Rheology of Igneous Melts at High Stresses and Strain Rates: Experimental Results for Rhyolite, Andesite, Basalt, and Nephelinite, *J. Geophys. Res.*, *95*, 15,695–15,701, 1990.

Williams, P., and S. Self, The October 1902 Plinian eruption of Santa Maria volcano, Guatemala, *J. Volcanol. Geotherm. Res.*, *16*, 1983.

Wylie, J., B. Voight, and J. Whitehead, Instability of Magma Flow from Volatile-Dependent Viscosity, *Science*, *285*, 1999.

Yokoyama, I., Geophysical characteristics of dacite volcanism 1977-1978 eruption of Usu volcano, *J. Volcanol. Geotherm. Res.*, *9*, 335–358, 1981.

Figure 1. a) Schematic representation of the plugged conduit model. Geometric and physical parameters are shown. No displacement in the direction perpendicular to the surface is allowed at the right and lower boundaries. The upper boundary is a free surface. The right boundary is situated far away from the conduit (at 100 km) in order to prevent boundary effects. Fluid flow is caused by pressure difference between the conduit bottom ($P = P_c$) and the surface ($P = 0$). A no-slip condition is applied at the fluid along the conduit wall. The continuity of the stress field, normal as well as tangential components, is applied at the conduit wall. The formation of the plug at the top of the conduit is modelled by an increase of the magma viscosity. b) 1-D viscosity profile used in our calculation (left side) and the resulting stresses (pressure and shear stress) at the conduit wall (right side). As a first approximation, the increase of the viscosity is modelled by a "step" function, with two extreme values: the viscosity in the magma column below the plug, μ_m, and the viscosity of the plug, μ_p. We consider an incompressible magma with constant density. In each sketch, dashed curves represented our reference case: the Poiseuille flow with a constant viscosity ($\mu = \mu_m$ at any depth).

Figure 2.

a) Mesh of the numerical model superimposed to the pattern of total displacements induced within the host rocks by a Poiseuille magma flow. The mesh is highly refined in the region close to the conduit, where the gradient of displacements are the largest. Displacements are induced by a flow at constant viscosity initiated by a pressure of 10 MPa at the bottom of a conduit. The conduit is a cylinder with a 15 m radius and a 5000 m length. Elastic parameters of the host rocks are respectively 4 GPa and 0.25 for the shear modulus G and the Poisson's ratio ν. Note that in lateral extension only the first 10 km of the 100 km corresponding to the actual box size, are shown. b) Zoom of the mesh in the 1 km^2 area near the surface corresponding to the red box of Figure a).

Figure 3. Surface displacements: radial (a), vertical (b) and tilt (c) induced by a constant viscosity magma flow (reference case chosen in the following). Displacements are obtained with respect to the lithostatic medium containing an overpressurized reservoir not connected to the surface with a Poisson's ratio equal to 0.25. Results are presented for three different conduit aspect ratio $(\frac{a_c}{L_c})$. Distances are normalized by the conduit length (L_c) and displacement by the ratio $(\frac{P_c}{G} L_c)$. The distance r=0 corresponds to the conduit wall. In each case, the total displacement (solid line) as well as displacement only induced by the shear stress component (short dashed) or by the pressure (large dashed) are shown.

Figure 4. Tilt induced by the formation of a plug at the top of the conduit, shown as a function of the two dimensionless numbers characterizing the plug: the length ratio ($\frac{h_p}{L_c}$) and the viscosity ratio ($\frac{\mu_p}{\mu_m}$). Tilt is calculated, at the surface, 500 m away from the conduit wall. Results are shown for a given conduit geometry, with a radius (a_c) of 15 m and a length (L_c) of 5000 m. The pressure P_c applied at the bottom is fixed at 10 MPa, the shear modulus of the host rocks, G, is equal to 0.8 GPa and the Poisson's ratio is set to 0.25. a) Part of the tilt which is only induced by the shear stress applied at the conduit wall. b) Part of the tilt which is only induced by the pressure applied at the conduit wall. Tilt represented in c) is the summation of the values shown in b) and c). The dashed line corresponds to the critical plug thickness, $h_{p(crit)}$, which gives the maximal tilt value for a given viscosity ratio. Note that tilt is relative to our reference case obtained with a constant viscosity magma flow, which means that tilt tends to zero when either h_p tends to zero or the viscosity ratio $\frac{\mu_p}{\mu_m}$ tends to 1.

Figure 5. Detection distance for the horizontal (a) and vertical (b) displacements as a function of the two dimensionless numbers related to the plug: the length ratio ($\frac{h_p}{L_c}$) and the viscosity ratio ($\frac{\mu_p}{\mu_m}$). The detection distance here corresponds to the maximal radial distance from the conduit wall where, respectively, a horizontal and a vertical displacement larger in amplitude than, respectively, one mm and 1 cm, is expected. The conduit length (L_c) and the pressure (P_c) applied at the bottom are, respectively, set to 5000 m and 10 MPa. The Poisson's ratio is set to 0.25 and $a_c = 15$ m and $G = 0.8$ GPa.

Figure 6. Detection distance for the tilt signal, function of the two dimensionless numbers related to the plug: the length ratio ($\frac{h_p}{L_c}$) and the viscosity ratio ($\frac{\mu_p}{\mu_m}$). The detection distance here corresponds to the maximal radial distance from the conduit wall where a tilt larger in amplitude than one microradian is expected. The conduit length (L_c) and the pressure (P_c) applied at the bottom are, respectively, set to 5000 m and 10 MPa. The Poisson's ratio is set to 0.25. Results are presented for four different cases: a) $a_c = 50$ m and $G = 0.8$ GPa b) $a_c = 50$ m and $G = 4.0$ GPa, c) $a_c = 15$ m and $G = 0.8$ GPa and d) $a_c = 15$ m and $G = 4.0$ GPa.

Figure 7. Relationship between tilt signal, magma flow rate and extrusion duration during the evolution of a plug within the volcanic conduit. Conditions are, as for Figure 4, obtained for a conduit radius (a_c) of 15 m, a conduit length (L_c) of 5000 m, a bottom pressure (P_c) of 10 MPa, a shear modulus (G) equal to 0.8 GPa and a Poisson's ratio (ν) set to 0.25. Two end-members for the plug evolution are tested: (1) a viscosity increase of plugs having a given thickness (left panels) ; (2) a thickness increase for plugs having a constant viscosity (right panels). For each case, we show a) Tilt calculated at a radial distance of 500 m from the conduit ; b) Normalized magma flow rate (Q/Q_{ref}) deduce from the expression (3) ; c) Extrusion duration in hours, which corresponds to the amount of time required to totally extrude the plug considered (with thickness h_p and viscosity μ_p). This parameter is directly inferred from the ratio between the volume of the plug ($\pi a_c^2 h_p$) and the magma flux Q, when the value of the magma viscosity μ_m is set. Here, the extrusion duration is obtained taking $\mu_m = 10^4$ Pa.s.

Figure 8. Amplitude of surface ground motion : a) the radial and b) vertical displacements as well as c) the tilt for various processes occurring on andesitic strato-volcanoes, detailed on sketch d). Numerical calculations are performed with the COMSOL software, taking a value of 0.8 GPa for rocks rigidity and 0.25 for the Poisson's ratio. The reference state is an overpressurized reservoir ($P_c = \rho_m g L_c$+10 MPa) embedded in a lithostatic medium, which feeds an open conduit with length (L_c) and radius (a_c) respectively equal to 5000 m and 15 m. Magma in the conduit has a constant viscosity (μ_m). Perturbations are the following: (1) Overpressure change of ΔP_c=1 MPa due to magma replenishment or withdrawal within a 10 km^3 spherical magma reservoir (long dashed curves in a-b-c). (2) Plug emplacement in the upper part of the conduit, characterised by a thickness (h_p) of 50 m and a viscosity ratio ($\frac{\mu_p}{\mu_m}$) equal to 10^5 (solid curves in a-b-c). (3) Load change of $P_d = 1$ MPa due to the construction/destruction of a 200 m radius (R_d) lava dome at the surface (short dashed curves in a-b-c). Note that the value of 1 MPa can be associated to a dome height variation of 60 m for eruptive products density of 1700 kg.m^{-3}.

Figure 9. a) Magma viscosity as a function of normalized depth (left side) and resulting stress components along the conduit wall (right side) for various models. Note that stress components represented are the differential terms compared to the lithostatic stress field. Black lines correspond to plug models described in our study. Four models are tested with the same viscosity contrast ($\frac{\mu_p}{\mu_m} = 10^5$) but different length ratio: $\frac{h_p}{L_c} = 0.01$, $\frac{h_p}{L_c} = 0.05$, $\frac{h_p}{L_c} = 0.10$ and $\frac{h_p}{L_c} = 0.25$. Red and blue lines correspond to calculation with more realistic profile for magma viscosity, which depends on the gas escape process occurring on the magma column. The first (red) is derived from *Sparks* [1997], where depth dependence of magma viscosity is expressed as a power-law function. The second (blue), deduced from the study of *Collombet* [2009], considers vertical gas loss as the previous, but also the lateral gas escape due to wall permeability. b) Tilt signal at the surface induced by the different flow models discussed in a). The reference state is the Poiseuille flow with a constant viscosity. The blue boxes indicate the tilt amplitude recorded in two andesitic volcanoes: (1) and (2) at Soufrière Hills (Montserrat) respectively in May-August 1997 and December 1996 [*Voight et al.*, 1998] ; (3) at Mt St Helens between July 2006 and January 2007 [*Anderson et al.*, 2010]. Parameters used for the calculation are the same as in Figure 4.

Figure 10. a) Evolution of the tilt calculated at 500 m from the conduit (black line) and the magma flow rate (grey line) during the plug thickness decrease. The viscosity ratio $\frac{\mu_p}{\mu_m}$ is fixed at 100. All parameters are the same as in Figure 7. The dots associated with numbers correspond to different cases of plug thickness, from 1 (very thick) to 4 (very thin). The last case, number 5, is related to a model without plug. b) Sketch showing the evolution of ground movement and magma flow rate during the decrease of a plug thickness. From case 3 to 4, we see a change in the direction of ground movement (inflation to subsidence) correlated with a strong increase of the magma flux. Both changes could be used as precursors in the eruption forecasting of andesitic volcanoes.

Figure 11. Analytic (solid lines) against numerical solutions (dots) for ground surface motion: a) the radial displacements induced by a pressurized conduit and b) the tilt induced by a vertical traction along the conduit wall. The conduit is a cylinder with a 15 m radius and a 5000 m length. Elastic medium is characterized by a shear modulus of 0.8 GPa and a Poisson's ratio of 0.25. In a), all the conduit is pressurized with a uniform pressure equal to 10 MPa. In b), the shear stress equal to 3000 Pa is applied in the lower part of the conduit, between -2500 and -5000 m depth. The bottom panels show for each case the relative difference in percent between analytic and numerical solutions.

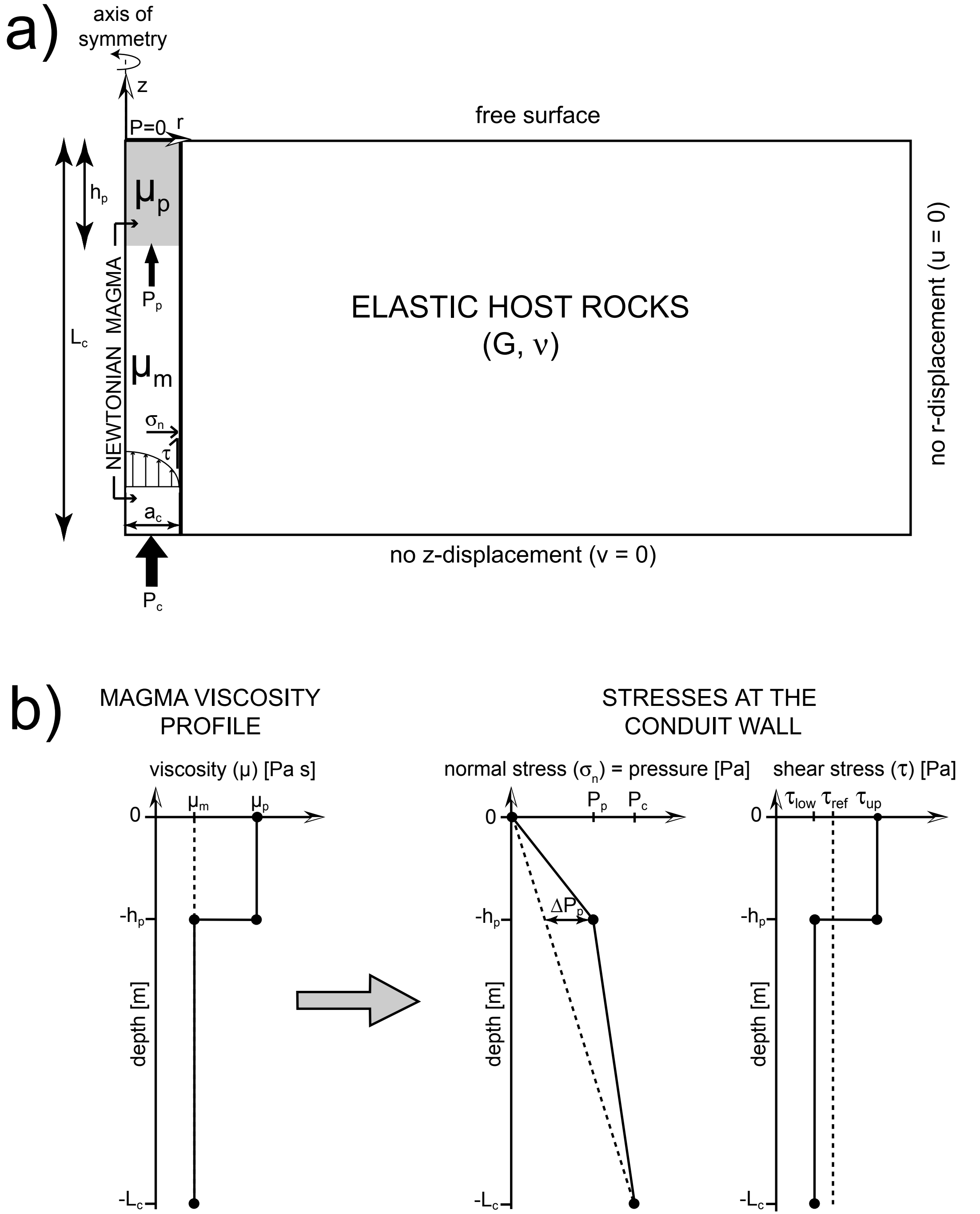
a)
axis of symmetry
z
P=0
r
free surface
h_p
μ_p
P_p
L_c
NEWTONIAN MAGMA
μ_m
σ_n
τ
a_c
P_c
ELASTIC HOST ROCKS
(G, ν)
no r-displacement (u = 0)
no z-displacement (v = 0)
b)
MAGMA VISCOSITY PROFILE
viscosity (μ) [Pa s]
0
μ_m
μ_p
$-h_p$
depth [m]
$-L_c$
STRESSES AT THE CONDUIT WALL
normal stress (σ_n) = pressure [Pa]
0
P_p
P_c
ΔP_p
$-h_p$
depth [m]
$-L_c$
shear stress (τ) [Pa]
0
τ_{low}
τ_{ref}
τ_{up}
$-h_p$
depth [m]
$-L_c$

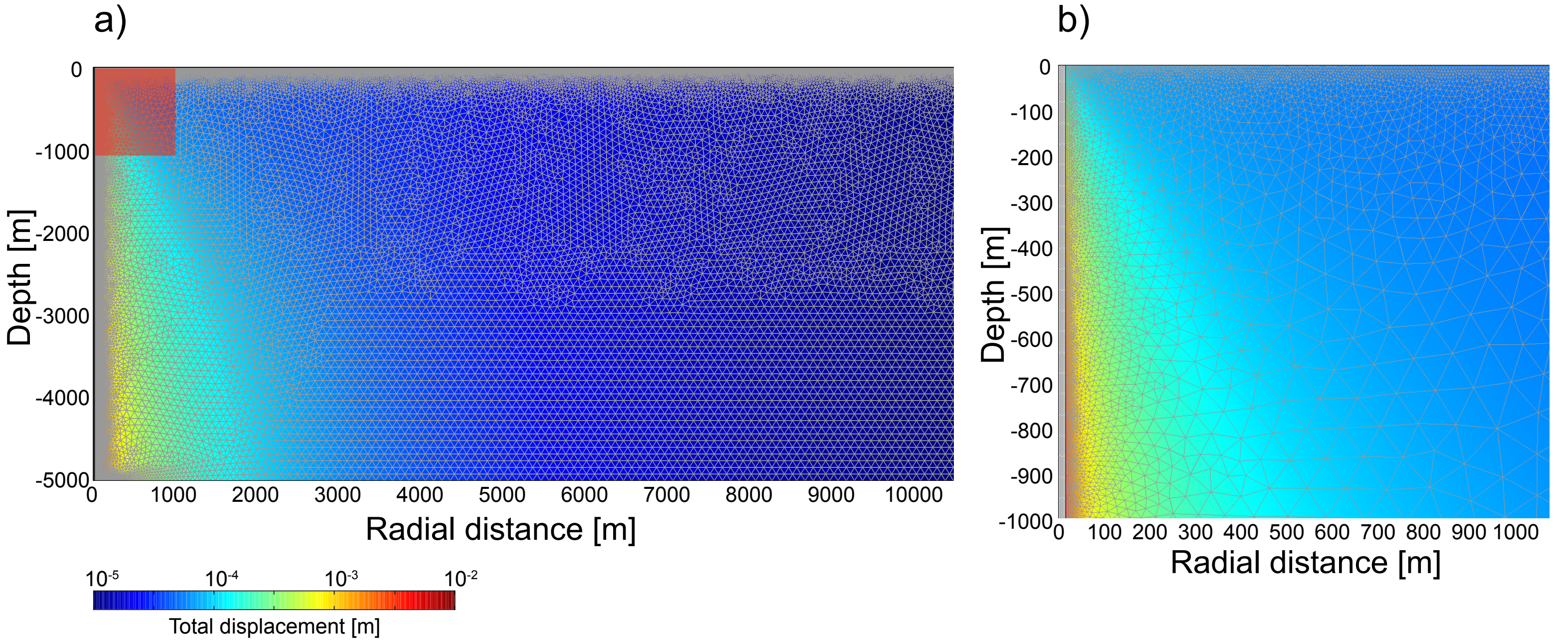

a)
b)
0
-1000
-2000
-3000
-4000
-5000
Depth [m]
0
1000
2000
3000
4000
5000
6000
7000
8000
9000
10000
Radial distance [m]
10^{-5}
10^{-4}
10^{-3}
10^{-2}
Total displacement [m]
0
-100
-200
-300
-400
-500
-600
-700
-800
-900
-1000
Depth [m]
0
100
200
300
400
500
600
700
800
900
1000
Radial distance [m]

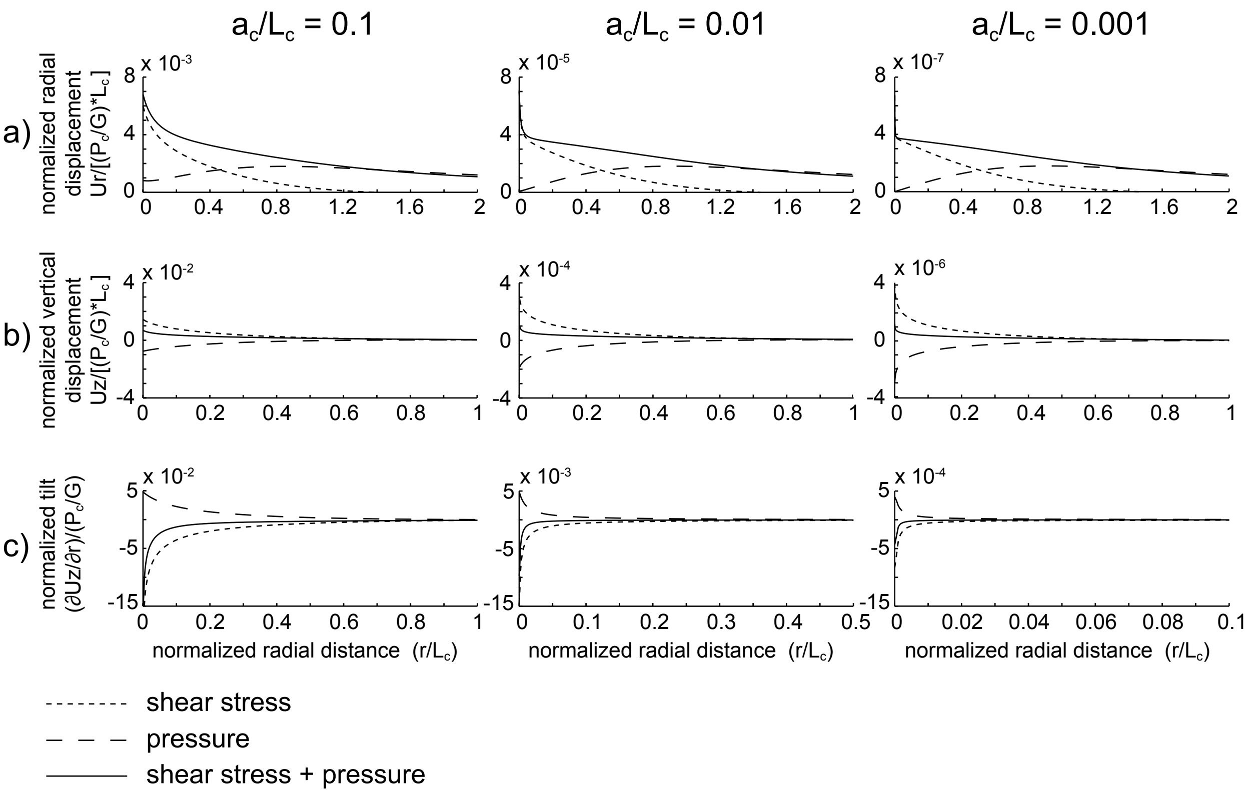

a_c/L_c = 0.1
a_c/L_c = 0.01
a_c/L_c = 0.001
a)
normalized radial displacement
$Ur/[(P_c/G)*L_c]$
x 10^{-3}
x 10^{-5}
x 10^{-7}
b)
normalized vertical displacement
$Uz/[(P_c/G)*L_c]$
x 10^{-2}
x 10^{-4}
x 10^{-6}
c)
normalized tilt
$(\partial Uz/\partial r)/(P_c/G)$
x 10^{-2}
x 10^{-3}
x 10^{-4}
normalized radial distance (r/L_c)
shear stress
pressure
shear stress + pressure

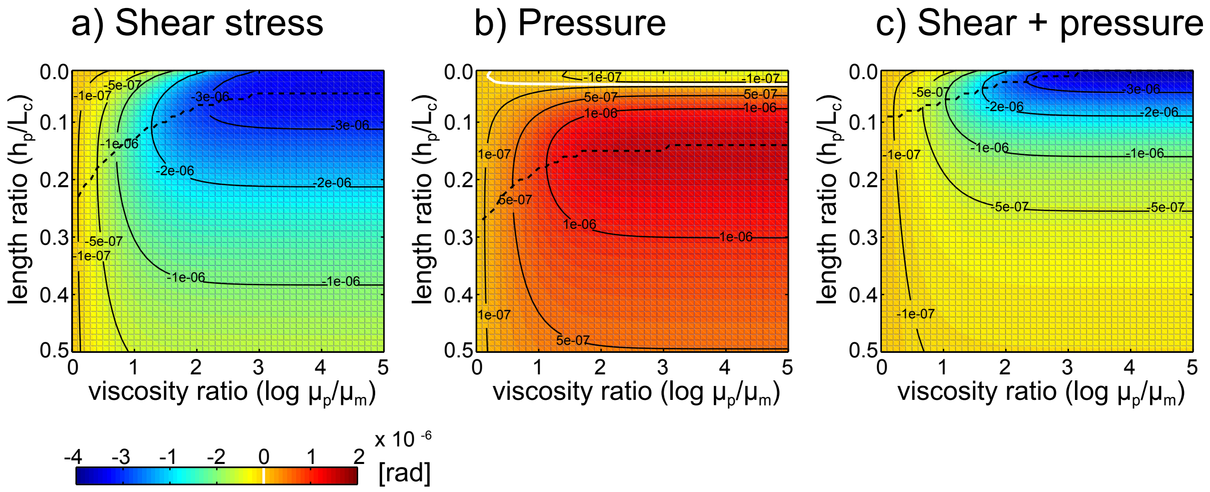

a) Shear stress
b) Pressure
c) Shear + pressure
length ratio (h_p/L_c)
viscosity ratio (log μ_p/μ_m)
-1e-07
-5e-07
-1e-06
-2e-06
-3e-06
1e-07
5e-07
1e-06
x 10 -6
[rad]

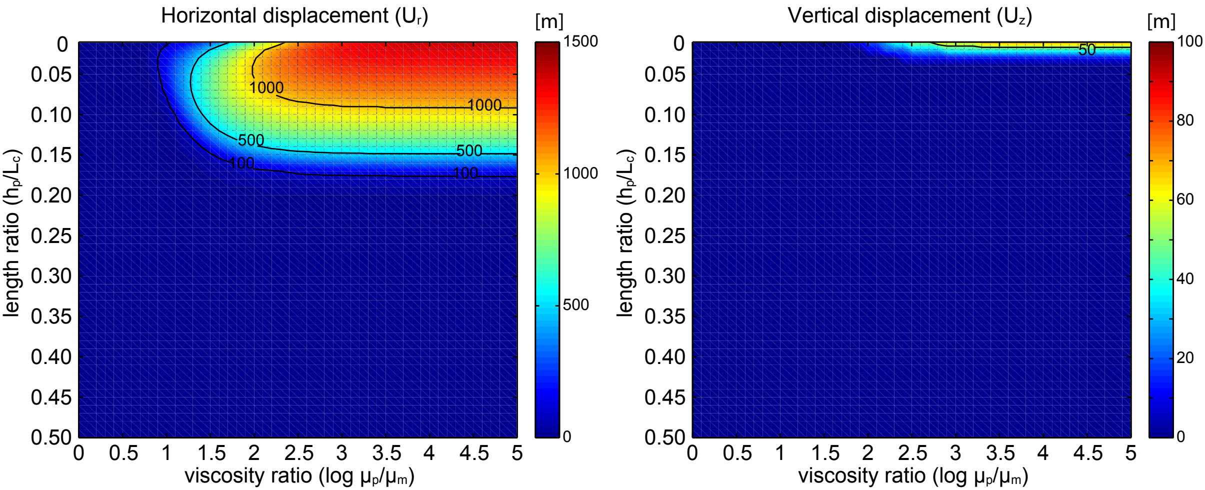
Horizontal displacement (U_r)
[m]
1500
1000
500
0
1000
1000
500
500
100
100
length ratio (h_p/L_c)
0
0.05
0.10
0.15
0.20
0.25
0.30
0.35
0.40
0.45
0.50
0
0.5
1
1.5
2
2.5
3
3.5
4
4.5
5
viscosity ratio (log μ_p/μ_m)
Vertical displacement (U_z)
[m]
100
80
60
40
20
0
50
length ratio (h_p/L_c)
viscosity ratio (log μ_p/μ_m)

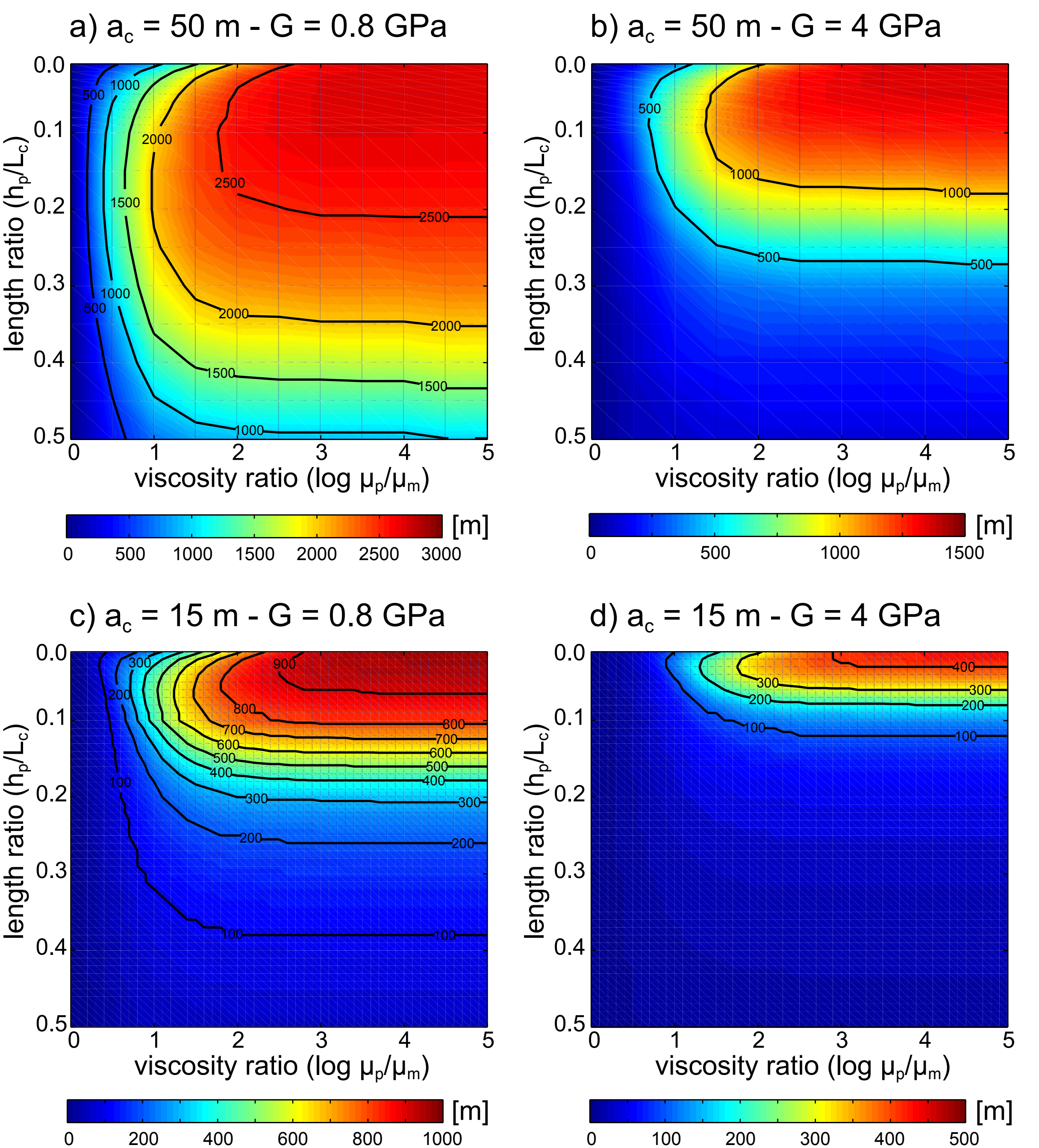
a) ac = 50 m - G = 0.8 GPa
b) ac = 50 m - G = 4 GPa
c) ac = 15 m - G = 0.8 GPa
d) ac = 15 m - G = 4 GPa
length ratio (hp/Lc)
viscosity ratio (log μp/μm)
[m]
0.0
0.1
0.2
0.3
0.4
0.5
0
1
2
3
4
5
0
500
1000
1500
2000
2500
3000
200
400
600
800
100
300

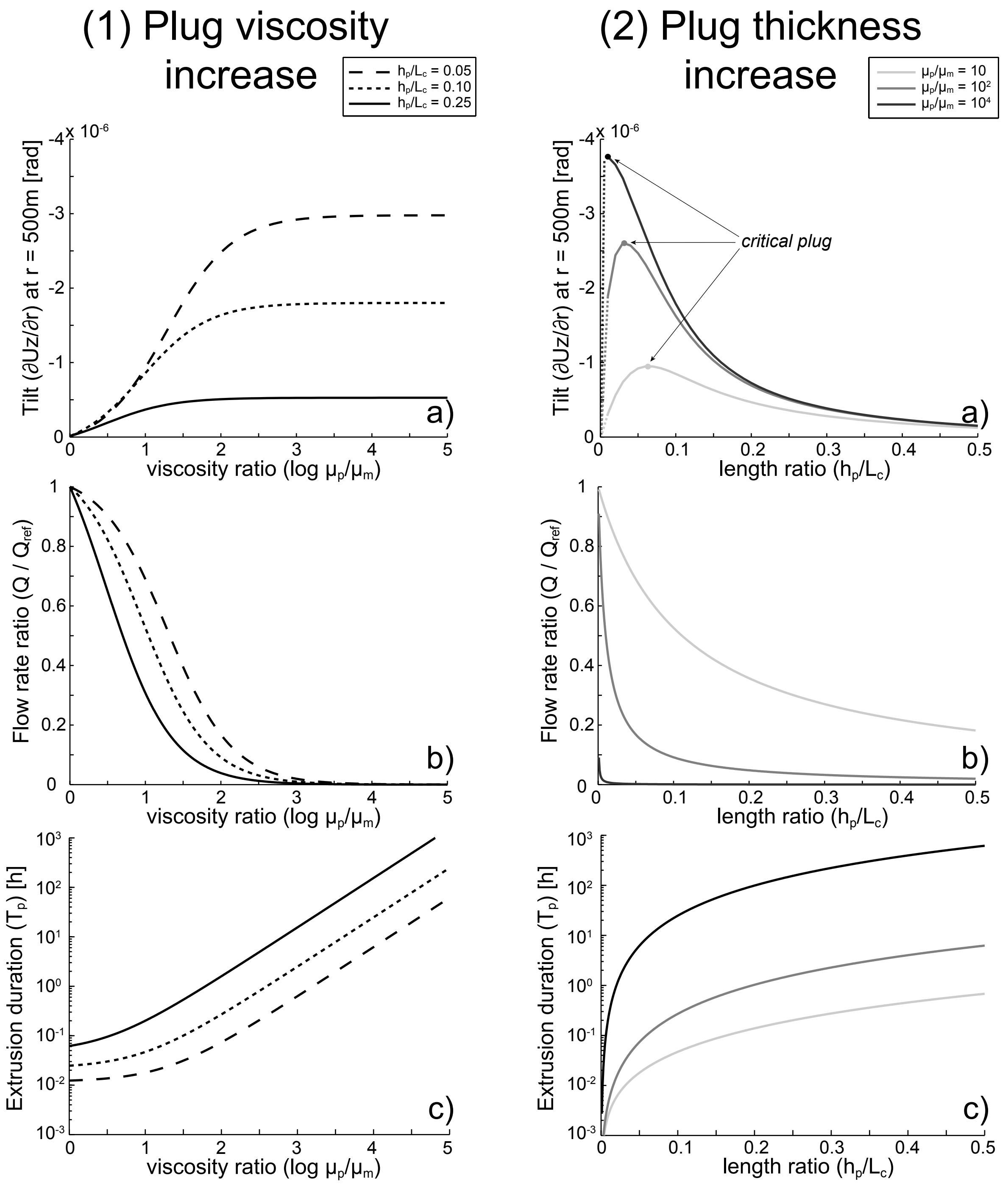

(1) Plug viscosity increase
(2) Plug thickness increase
hp/Lc = 0.05
hp/Lc = 0.10
hp/Lc = 0.25
μp/μm = 10
μp/μm = 10²
μp/μm = 10⁴
x 10-6
Tilt (∂Uz/∂r) at r = 500m [rad]
critical plug
viscosity ratio (log μp/μm)
length ratio (hp/Lc)
Flow rate ratio (Q / Qref)
Extrusion duration (Tp) [h]
a)
b)
c)

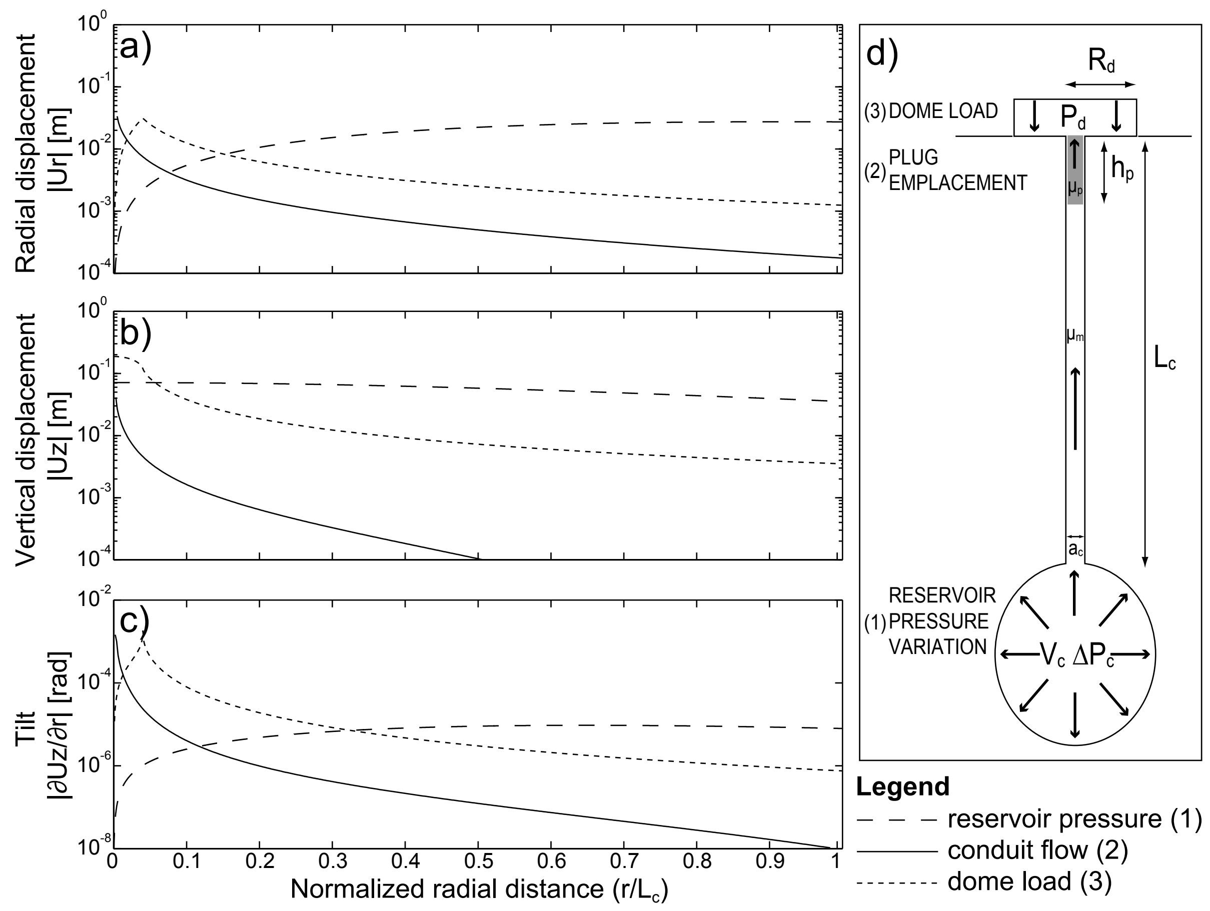
a)
b)
c)
d)
Radial displacement |Ur| [m]
Vertical displacement |Uz| [m]
Tilt |∂Uz/∂r| [rad]
Normalized radial distance (r/Lc)
0 0.1 0.2 0.3 0.4 0.5 0.6 0.7 0.8 0.9 1
Rd
(3) DOME LOAD
Pd
(2) PLUG EMPLACEMENT
hp
μp
μm
Lc
ac
(1) RESERVOIR PRESSURE VARIATION
Vc ΔPc
Legend
reservoir pressure (1)
conduit flow (2)
dome load (3)

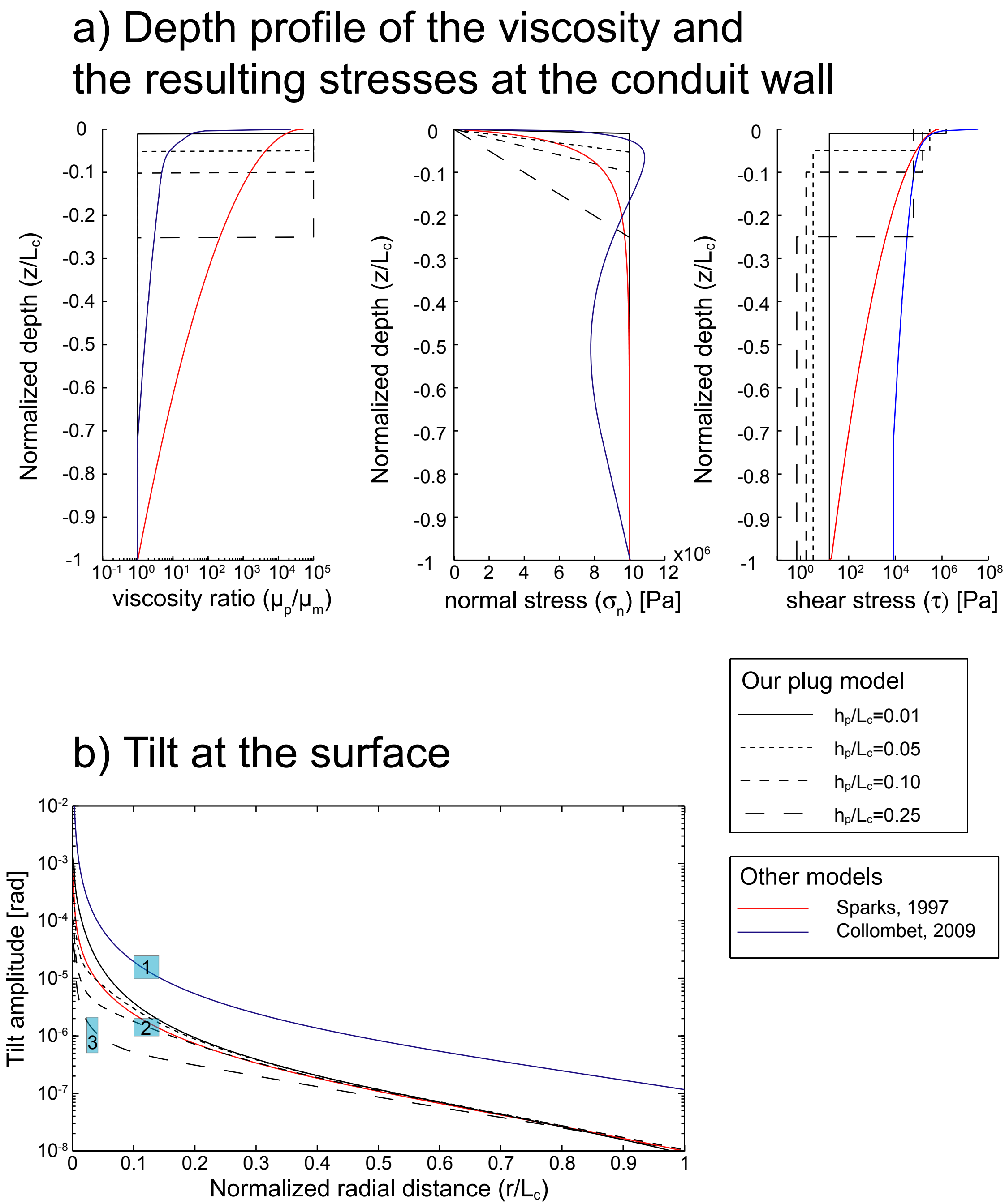

a) Depth profile of the viscosity and the resulting stresses at the conduit wall
Normalized depth (z/Lc)
viscosity ratio (μp/μm)
normal stress (σn) [Pa]
x10^6
shear stress (τ) [Pa]
b) Tilt at the surface
Tilt amplitude [rad]
Normalized radial distance (r/Lc)
1
2
3
Our plug model
hp/Lc=0.01
hp/Lc=0.05
hp/Lc=0.10
hp/Lc=0.25
Other models
Sparks, 1997
Collombet, 2009

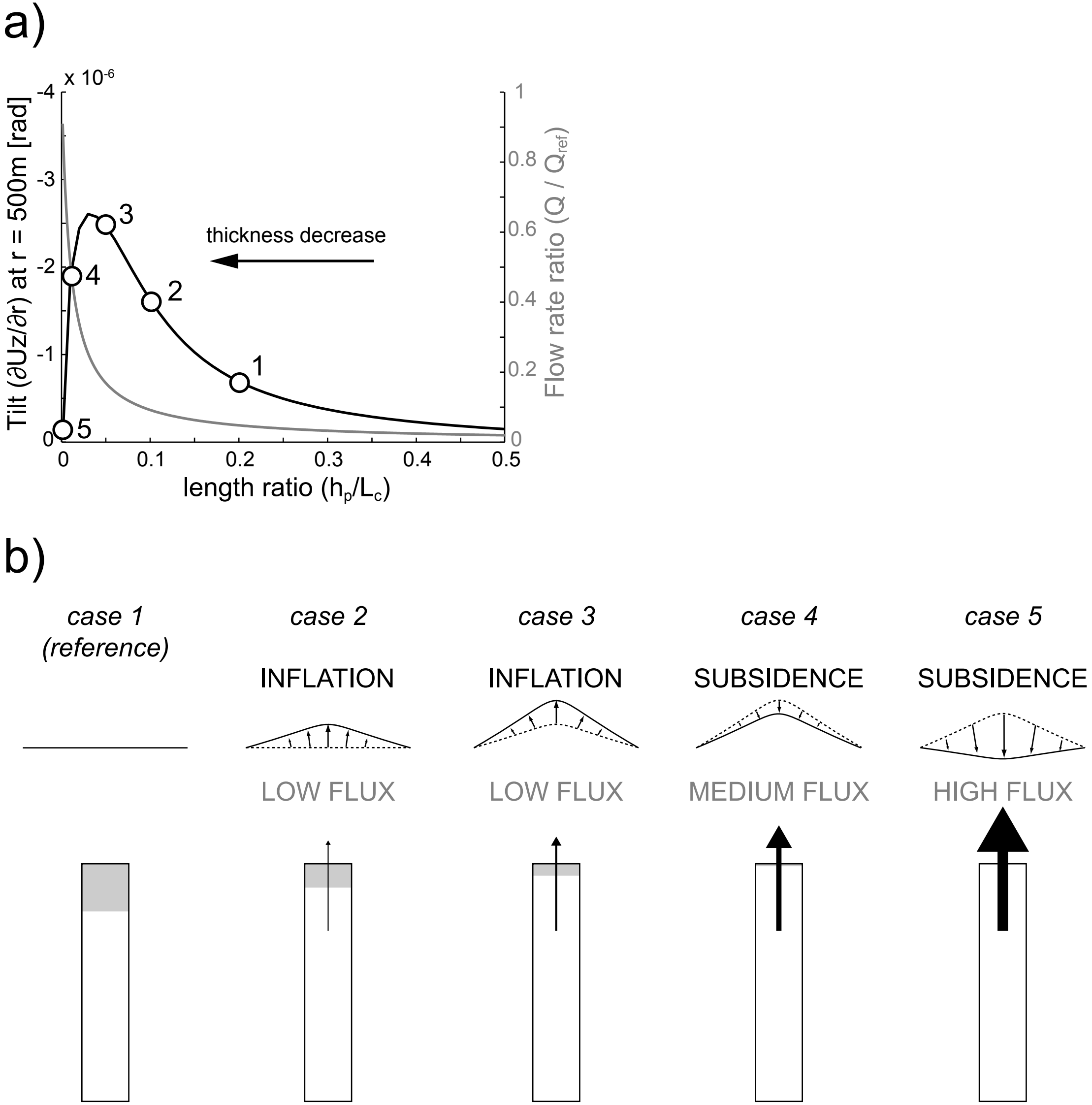

a)
x 10-6
Tilt (∂Uz/∂r) at r = 500m [rad]
-4
-3
-2
-1
0
1
0.8
0.6
0.4
0.2
0
Flow rate ratio (Q / Qref)
thickness decrease
1
2
3
4
5
0
0.1
0.2
0.3
0.4
0.5
length ratio (hp/Lc)
b)
case 1
(reference)
case 2
case 3
case 4
case 5
INFLATION
INFLATION
SUBSIDENCE
SUBSIDENCE
LOW FLUX
LOW FLUX
MEDIUM FLUX
HIGH FLUX

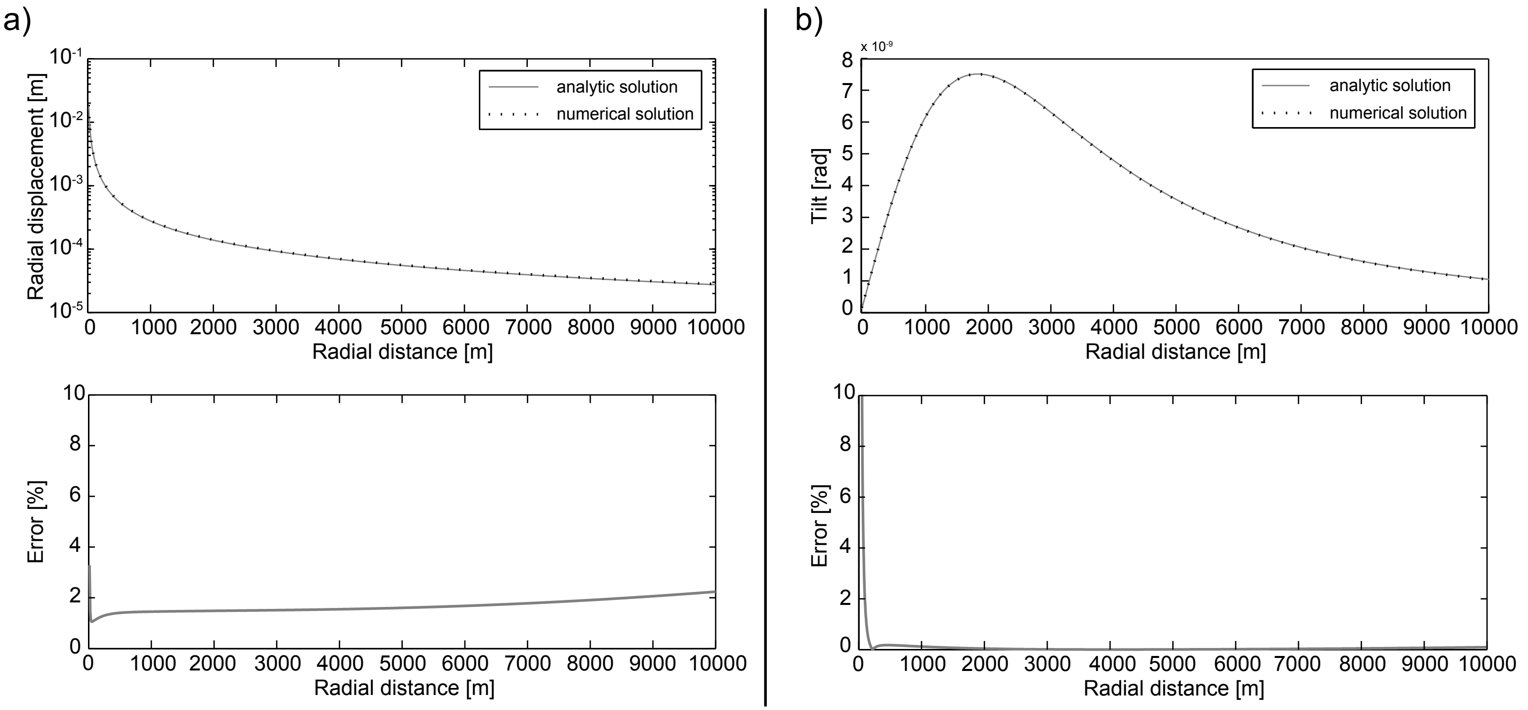

a)
Radial displacement [m]
analytic solution
numerical solution
Radial distance [m]
Error [%]
Radial distance [m]
b)
x 10-9
Tilt [rad]
analytic solution
numerical solution
Radial distance [m]
Error [%]
Radial distance [m]